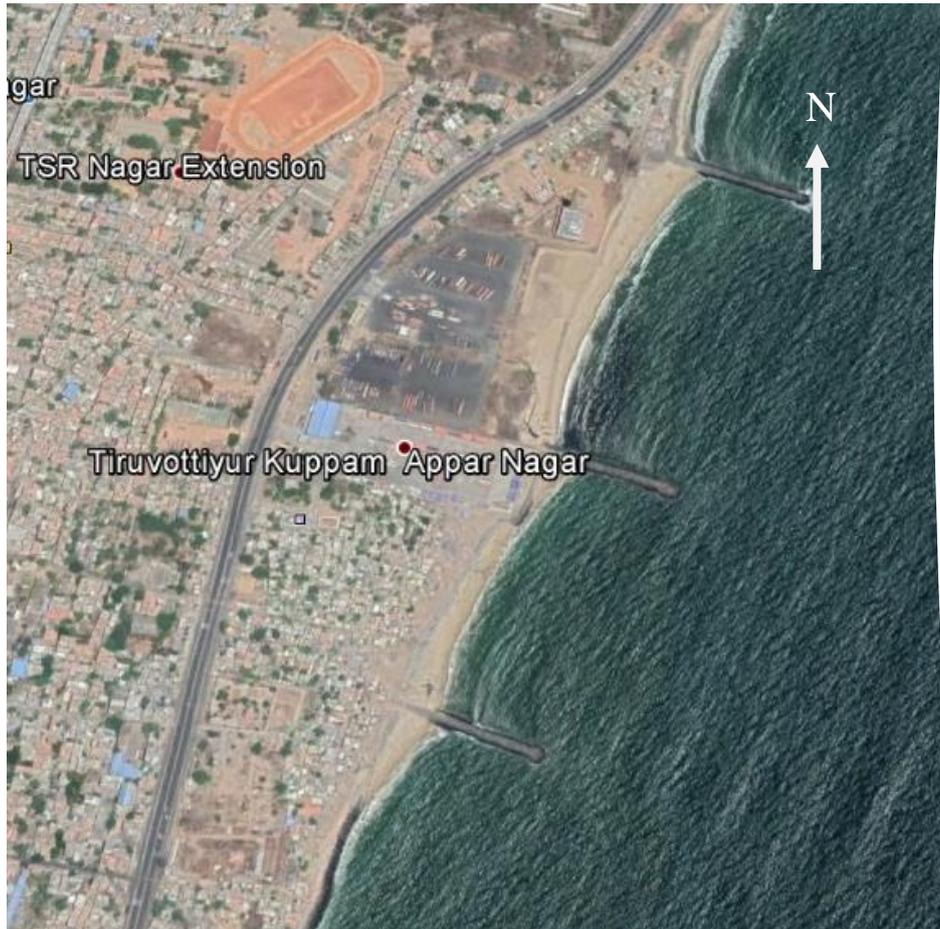# TUNA Fishing Harbor at Thiruvottriyur Kuppam

Report Submitted to
Fisheries Department
Tamil Nadu.

By,
Prof. V. Sundar
Prof. S.A. Sannasiraj

Department of Ocean Engineering
Indian Institute of Technology Madras
Chennai 600 036, India.
July 2019

CONTENTS

TABLES

FIGURES

PLATES

1.0 INTRODUCTION

The coastal area, adjoining the north of the Chennai Port has been adversely affected by continued erosion due to the development of the port. Since several developmental activities such as advent of industries, improvement of fisheries, etc. a groyne field was constructed stretching from Royapuram to northwards and the sea wall stretch of about 10 km length lying parallel to Ennore High Road to combat the erosion problems. A proposal was further made to expand existing groynes to form a fishing harbor. The Fisheries Department, Chennai requested the Department of Ocean Engineering, IIT Madras to revise/revive the proposed layout and perform numerical model studies to validate the same. Therefore, the layout was revised and subjected to tranquility and shoreline evolution studies, which is detailed in this report.

2.0 SCOPE AND OBJECTIVES

The main objective of the study is to revise the layout of the proposed fishing harbor The scope of the study includes,

- To prevent erosion of shoreline and ascertain development of fisheries related activities along the coast.
- To suggest suitable extension for groynes to form a pair of breakwaters and predict the shoreline behavior in view of the proposed groins through numerical modeling.
- Numerical model study for the wave transformation/tranquility due to the extension of the existing shore connected structures, and to determine the operability of vessels.

3.0 WAVE CHARACTERISTICS
3.1 General

The National Institute of Oceanography (1990) published a wave atlas for Arabian Sea and Bay of Bengal (Latitude: $0^0 – 25^0$ N and Longitude: $60^0 – 95^0$ E) compiling the ship observed data for 19 years from 1968 to 1986. The coastal region around India is divided into 10 grids, each of size 5^0 latitude and 5^0 longitudes as shown in **Fig. 2.** The grids 1 to 4 falls in the Bay of Bengal on the east coast, grids 5 to 7 fall in Indian Ocean in the south and grids 8 to 10 all in the Arabian Sea on the west coast. The present study area comes under the grid located at $5 – 10^0$ N and $75 – 80^0$ E in the wave atlas, representing grid number six. The wave

data (wave height, wave period and wave direction) from wave atlas given for deep-waters were used for the present study.

3.2 Wave height

The monthly distribution of deep-water wave heights in terms of percentage of occurrence derived from wave rose diagrams are projected in **Figs. 3 to 6.** The class interval adopted for the calculations is 0.5m. It is observed from the results, that the most frequently occurring wave height is about 1.5m with a percentage of occurrences of 20 to 30% for the months January and November. From the above referred figures, it is also observed that the most frequently occurring wave height is 1.0m with a percentage of occurrences of 20 to 35% during the months of February, March, April, May, October and December. The most frequently occurring wave height is 2m with a percentage of occurrences between 25 to 35% for the months June to September.

3.3 Wave periods

The monthly distribution of wave periods in terms of percentage of occurrence derived from the wave atlas is projected in **Figs. 7 to 10**. The class interval adopted for the presentation is 1sec. From the above figure, it is observed that the maximum percentage of occurrence is the waves associated with periods ranging between 5 and 6 seconds.

3.4 Wave direction

The monthly distribution of wave directions with respect to geographic north in terms of percentage of occurrence obtained from the wave atlas is projected in **Figs. 11 to 14**. The class interval adopted for the presentation is 20^0. The average wave characteristics given as the input to the numerical model is as per given in **Table 1.** The shore-normal angle for the present study was arrived to be 218° with respect to geographic north.

Table 1: Wave characteristics for the present study

Month	Deep water Wave direction w.r.t North ($\theta°$)	Wave height (m)	Wave period (sec), T	Wave direction from shore normal ($\theta°$) in
January	60^0	1.5	5	49^0
February	60^0	1.0	5	49^0
March	90^0	1.0	5	19^0

April	150^0	0.5	5	-41^0
May	180^0	1.0	5	-71^0
June	180^0	2.0	5	-71^0
July	180^0	1.0	5	-71^0
August	180^0	2.0	5	-71^0
September	180^0	1.0	6	-71^0
October	60^0	1.0	5	49^0
November	60^0	1.0	6	49^0
December	30^0	2.0	6	79^0

4.0 LITTORAL DRIFT ESTIMATE

4.1 Distribution of Sediment Transport

The wave atlas data has been analyzed to obtain the monthly averaged wave height, wave period and wave direction. These are offshore wave climate and are transformed to the near shore location of Thiruvottriyur Kuppam coast using Snell's law. The average breaking wave characteristics were derived from the available wave data. The monthly distribution of mean breaker wave height for the study area is shown in **Fig. 15(a).** The results indicate that the mean breaker height varies from about 0.87m to 1.57m. The breaker height is observed to be a maximum during June and July. The monthly distribution of the mean breaker wave angle with respect to shore normal is shown in **Fig. 15(b).** From the results it is seen that for the study area, the breaker angle with respect to shore normal and long shore current velocity are directed towards South from October to February. The average surf width in which the long shore drift is predominant is further estimated from the breaker wave height for the given bathymetry and is projected in **Fig.15(c)** for the different months. It shows that the maximum surf width of about 95m occurs during the months of June and July. Further, the derived wave characteristics were used to calculate the long shore sediment transport. Three different methods CERC (1984), Komar (1976a), and by integrating the distribution across the surf zone (Komar, 1976b) have been adopted to calculate the alongshore sediment transport rate. The average sediment transport rate for the different months is shown in

Fig.16. All the three methods have yielded similar order sediment transport rate. The net drift is found to be about 400000m^3 per annum and directed towards the North.

5.0 PROPOSED SCHEME

In view of promoting fisheries in the vicinity of the coast of Thiruvottriyur Kuppam, the existing groynes are planned to be extended to form a pair of breakwaters, thereby proving calm tranquil conditions for landing of fishing boats. The northern breakwater extends for about 510 m unitl -6 m water depth and the southern breakwater extends upto -7.5m water depth. An opening width of 90 m is provided between the base of northern and southern breakwater for movement of fishing boats. The layout is shown in **Plate 1**.

The tranquil conditions within the fishing harbour basin were studied for operability. Furthermore, the proposed coastal protection scheme has been further examined for shoreline evolution using numerical modeling techniques, which supplements our understanding of the shoreline behavior.

6.0 NUMERICAL MODELLING FOR SHORELINE EVOLUTION

6.1 General

Structures in the near shore environment are built for different purposes. These may be for the formation of artificial harbors, shore protection measures, seawater intake systems, disposal of effluent, etc. There are several configurations of such structures with respect to the shoreline, among which, structures normal to the shore is most common. The construction of a shore-connected structure often leads to changes in the shoreline. This warrants a study on the shoreline due to presence of the shore-connected structures. Such a study is very much essential in planning stage; so as to assess the impact of shore connected structures on the adjacent shoreline.

Numerical models offer the capability to study the effect of the wave characteristics, structure dimensions and other associated parameters in providing reasonable estimates of the shoreline response. As the ocean waves approaches the near shore it undergoes transformations like shoaling, refraction, diffraction and breaking. The phenomena of wave breaking throw sediments to the surface due to the turbulence generated. The sediments in suspension are then driven by the wave-induced currents. Since the direction of waves in the

near shore is oblique, the currents induced by them have two components. One along the shore called long shore current mainly responsible for the long shore sediment transport, which plays an important role in the shoreline changes especially due to the shore connected structures. The other component is in the direction normal to the shore, in which case, the mode of sediment transport is called onshore-offshore sediment transport. When a structure normal to the shoreline is constructed, it will intercept the free passage of long shore sediment transport, which results an imbalance in the quantity of sediment in the near shore especially near the structure. This leads to accretion on the updrift side and erosion on the downdrift side of the structure.

6.2 Methodology

KRAUS and HARIKAI (1983) proposed a numerical scheme to solve the one line model using Crank Nicholson implicit finite difference method. The non-dimensional equation of shoreline

$$y^*_{n,t^*+1} = B\{Q^*_{n,t^*+1} - Q^*_{n+1,t^*+1}\} + C_n \tag{1}$$

$$where\ B = \frac{\delta t^*}{2 \times \delta x^*}\ and\ C_n = B\{Q^*_{n,t^*} - Q^*_{n+1,t^*} + 2\delta x^* q^*_{n,t^*}\} + y^*_{n,t^*} \tag{2}$$

The non-dimensional shoreline is divided into 'n' grid points at equal non-dimensional interval, δx^*. Then shoreline changes over a non-dimensional time, δt^* is calculated using Crank-Nicholson finite difference scheme. The schematic diagram for finite difference scheme is shown in **Fig. 17.**

In this method, Q^* at the time interval ($t^* + 1$) is expressed in terms of the shoreline co-ordinate of y*, first isolating the term involving α_{sp} (angle of shoreline normal to x-axis) using trigonometric identities. One of the term involving α_{sp} is then expressed as first order quantities in y* at time step (t*+1).

$$Q^* = K_D^2 \cos(\alpha_o) \sin(\alpha_b) \tag{3}$$

Where, $\alpha_o = \alpha - \alpha_{sp}$ and α is wave direction with respect to x-axis. The definition sketch showing the angles is shown in **Fig. 18.**

The elliptical form of mild slope equation, which deals with combined refraction-diffraction,

$$Q^* = K_D^2 \cos\left(\alpha - \alpha_{sp}\right)\sin\left(\alpha_b\right) \qquad (4)$$

$$Q^* = K_D^2 \sin\left(\alpha_b\right)\left\{\cos\left(\alpha\right)\sin\left(\alpha_{sp}\right)\cot\left(\alpha_{sp}\right) + \sin\left(\alpha\right)\sin\left(\alpha_{sp}\right)\right\} \qquad (5)$$

$$Q^* = E_n\left\{y_{n-1,t^*+1} - y^*_{n,t^*+1}\right\} + F_n \qquad (6)$$

Where $E_n = K_D^2\{\cos(\alpha)\sin(\alpha_{sp,t^*})\sin(\alpha_{b,t^*})\}/\delta x^*$ *and* $F_n = K_D^2\{\sin(\alpha_{sp,t^*})\sin(\alpha_{b,t^*})\}$

By substituting above equations, give the final equation as given below

$$BE_n Q^*_{n-1,t^*+1} - (1+2BE_n)Q^*_{n,t^*+1} + BE_n Q^*_{n+1,t^*+1} = E_n[C_n - C_{n-1}] - F_n \qquad (7)$$

The above equations represent a set of (N-1) linear equation for (N-1) unknowns. The end values are specified as boundary conditions, that is, $Q^*_1 = 0$ and $Q^*_{N+1} = Q^*_N$. The above equation results into a tridiagonal form which is solved for Q^*. This process is repeated for the entire duration and non-dimensional quantity is converted into real quantities using the corresponding scale factors. The program has been validated with published results.

6.3 Input and Output from the numerical model

The coastal line is discretized into number of grids with an equal spacing of 5m. The co-ordinates of the existing shoreline were provided. The length of the structure andgrain size of the sediments (0.2mm) required for the calculation of active depth of the sediment transport and water depth at the tip of the structure are the inputs given to the model. In addition to these, the monthly wave characteristics and the number of years over which the shoreline change is desired to be mentioned.

The output shows the predicted shoreline changes after a period of 1, 5, 10, 15, 20& 25 years. The upstream of the structures shows advancement of the shoreline position, while, the downstream end shows the erosion.

6.4 Results and discussion

The numerical model to predict the shoreline evolution due to the shore-connected structures has been used to predict the shoreline changes due to the proposed groins. The

wave characteristics given as the inputs to the numerical model is as per given above table.In addition, the length of the groins, water depth at the end of the groins and the present status of the shore are also to be given as the inputs to the numerical model.

The numerical model was executed for the most frequently occurring wave characteristics for the different months as stated earlier**.** The result on the predicted shoreline variations over years are projected in **Fig. 19**. The shoreline prediction has been made at the end of 1 year, 5 years, 10 years, 15 years, 20 years and 25 years after the construction of the groins and has been presented by superimposing the shoreline patterns. The results also show that no significant erosion is observed on either side of the proposed shore protections measure.

7.0 WAVE TRANQUILLITY STUDY

7.1 Offshore wave characteristics

The wave characteristics such as significant wave height, mean wave period and mean wave direction at a deep-water location (13°15'0.00"N, 80°30'0.00"E) off Thiruvottiyur Kuppam have been extracted from the ECMWF (European Centre for Medium-Range Weather Forecasts) including the wind-wave modeling hind-cast studies. The data are sampled at every 6 hours. Basically, the wave field follows the wind pattern. It is noted that the spatial variability is closely related, the maximum of H_s are associated with maximum wind speeds. The offshore wave climate for an annual year is presented in **Fig.20**.The joint distribution tables of significant wave height vs. wave direction, Mean wave period vs. mean wave direction and significant wave height vs. mean wave period are presented in **Tables 2**, **3** and **4** respectively.The waves are predominantly observed in 6s to 8s period with the significant wave height ranges between 0.5m to 1.5m. However, larger wave heights were also observed.

Table 2. Wave height vs Mean direction joint distribution

Wave direction	Wave Height (m)										Total
	0-0.5	0.5-1	1-1.5	1.5-2	2-2.5	2.5-3	3-3.5	3.5-4	4-4.5	4.5-5	
N-NNE	0.00	0.00	0.00	0.00	0.00	0.00	0.00	0.00	0.00	0.00	**0.00**
NNE-NE	0.00	0.07	0.34	0.00	0.00	0.00	0.00	0.00	0.00	0.00	**0.41**
NE-NEE	0.00	2.06	1.44	0.21	0.00	0.00	0.00	0.00	0.00	0.00	**3.70**
NEE-E	0.00	7.68	6.99	0.00	0.00	0.00	0.00	0.00	0.00	0.00	**14.67**
E-SEE	0.00	5.83	2.54	0.00	0.00	0.00	0.00	0.00	0.00	0.00	**8.36**
SEE-SE	0.07	3.36	1.30	0.00	0.00	0.00	0.00	0.00	0.00	0.00	**4.73**
SE-SSE	0.00	10.14	1.10	0.00	0.00	0.00	0.00	0.00	0.00	0.00	**11.24**
SSE-S	0.00	24.13	16.38	0.34	0.00	0.00	0.00	0.00	0.00	0.00	**40.85**
S-SSW	0.14	6.99	4.46	0.00	0.00	0.00	0.00	0.00	0.00	0.00	**11.85**
SSW-SW	0.00	1.23	0.82	0.07	0.00	0.00	0.00	0.00	0.00	0.00	**2.12**
SW-SWW	0.00	0.75	0.00	0.00	0.00	0.00	0.00	0.00	0.00	0.00	**0.75**
SWW-W	0.07	0.07	0.07	0.00	0.00	0.00	0.00	0.00	0.00	0.00	**0.21**
W-NWW	0.00	0.48	0.00	0.00	0.00	0.00	0.00	0.00	0.00	0.00	**0.48**
NWW-NW	0.07	0.14	0.00	0.00	0.00	0.00	0.00	0.00	0.00	0.00	**0.21**
NW-NNW	0.00	0.27	0.07	0.00	0.00	0.00	0.00	0.00	0.00	0.00	**0.34**
NNW-N	0.00	0.07	0.00	0.00	0.00	0.00	0.00	0.00	0.00	0.00	**0.07**
Total	**0.34**	**63.26**	**35.77**	**0.62**	**0.00**	**0.00**	**0.00**	**0.00**	**0.00**	**0.00**	**100.00**

Table 3. Wave Period vs Mean direction joint distribution

Wave direction	Wave Period (s)											Total
	0-2	2-4	4-6	6-8	8-10	10-12	12-14	16-18	18-20	20-22	22-24	
N-NNE	0.00	0.00	0.00	0.00	0.00	0.00	0.00	0.00	0.00	0.00	0.00	**0.00**
NNE-NE	0.00	0.00	0.41	0.00	0.00	0.00	0.00	0.00	0.00	0.00	0.00	**0.41**
NE-NEE	0.00	0.00	3.22	0.34	0.14	0.00	0.00	0.00	0.00	0.00	0.00	**3.70**
NEE-E	0.00	0.07	13.16	1.44	0.00	0.00	0.00	0.00	0.00	0.00	0.00	**14.67**
E-SEE	0.00	0.00	6.37	1.99	0.00	0.00	0.00	0.00	0.00	0.00	0.00	**8.36**
SEE-SE	0.00	0.00	1.92	2.54	0.27	0.00	0.00	0.00	0.00	0.00	0.00	**4.73**
SE-SSE	0.00	0.00	3.02	7.54	0.69	0.00	0.00	0.00	0.00	0.00	0.00	**11.24**
SSE-S	0.00	0.00	13.71	21.45	5.41	0.27	0.00	0.00	0.00	0.00	0.00	**40.85**
S-SSW	0.00	0.00	6.17	4.66	0.75	0.00	0.00	0.00	0.00	0.00	0.00	**11.85**
SSW-SW	0.00	0.00	2.06	0.07	0.00	0.00	0.00	0.00	0.00	0.00	0.00	**2.12**
SW-SWW	0.00	0.07	0.69	0.00	0.00	0.00	0.00	0.00	0.00	0.00	0.00	**0.75**
SWW-W	0.00	0.07	0.14	0.00	0.00	0.00	0.00	0.00	0.00	0.00	0.00	**0.21**
W-NWW	0.00	0.21	0.27	0.00	0.00	0.00	0.00	0.00	0.00	0.00	0.00	**0.48**
NWW-NW	0.00	0.21	0.00	0.00	0.00	0.00	0.00	0.00	0.00	0.00	0.00	**0.21**
NW-NNW	0.00	0.14	0.21	0.00	0.00	0.00	0.00	0.00	0.00	0.00	0.00	**0.34**
NNW-N	0.00	0.00	0.07	0.00	0.00	0.00	0.00	0.00	0.00	0.00	0.00	**0.07**
Total	**0.00**	**0.75**	**51.68**	**40.03**	**7.27**	**0.27**	**0.00**	**0.00**	**0.00**	**0.00**	**0.00**	**100.00**

Table 4. Wave height vs mean period joint distribution

Hs (m)	Tm (s)												Total
	2	4	6	8	10	12	14	16	18	20	22	24	
0.5	0.00	0.00	0.00	0.00	0.00	0.00	0.00	0.00	0.00	0.00	0.00	0.00	0.00
1	0.14	0.62	0.00	0.00	0.00	0.00	0.00	0.00	0.00	0.00	0.00	0.00	0.75
1.5	0.07	35.44	15.90	0.21	0.00	0.00	0.00	0.00	0.00	0.00	0.00	0.00	51.61
2	0.14	25.02	14.80	0.14	0.00	0.00	0.00	0.00	0.00	0.00	0.00	0.00	40.10
2.5	0.00	2.47	4.59	0.21	0.00	0.00	0.00	0.00	0.00	0.00	0.00	0.00	7.27
3	0.00	0.00	0.21	0.07	0.00	0.00	0.00	0.00	0.00	0.00	0.00	0.00	0.27
3.5	0.00	0.00	0.00	0.00	0.00	0.00	0.00	0.00	0.00	0.00	0.00	0.00	0.00
4	0.00	0.00	0.00	0.00	0.00	0.00	0.00	0.00	0.00	0.00	0.00	0.00	0.00
4.5	0.00	0.00	0.00	0.00	0.00	0.00	0.00	0.00	0.00	0.00	0.00	0.00	0.00
5	0.00	0.00	0.00	0.00	0.00	0.00	0.00	0.00	0.00	0.00	0.00	0.00	0.00
Total	0.34	63.54	35.50	0.62	0.00	0.00	0.00	0.00	0.00	0.00	0.00	0.00	100.00

7.2 Numerical modelling

The study aims at providing an depth analysis on the wave tranquility near the proposed groyne field at Thiruvottiyur Kuppam. A suitable numerical model is required in order to carry out this task. For the present simulation, the well known CGWAVE model has been used.

The nonlinear wave propagation associated with most of the observed phenomenon in offshore region (e.g., wave reflection, refraction and diffraction) is generally represented by the shallow water mild slope equation.

$$\nabla.\left(C_p C_g \nabla \eta\right) + k^2 C_p C_g \eta = 0 \qquad (8)$$

Where, C_p and C_g are the wave celerity and group celerity respectively. η is the water surface elevation. k is the wave number. For the computation of near shore wave field, this model

(Eqn. (8)) is subjected to the proper boundary conditions. This is provided by the bathymetry and the shore line.

The computational domain roughly approximates a semi circle of radius 2.8 km. **Fig.21** shows the domain where the computations are actually performed. The direction of the incident monochromatic wave is defined with respect to the geometric northern direction.

A numerical method is required to solve the above Eqn. (8) for wave elevation. In this study, Finite Element Method (herein after abbreviated as FEM) is employed. This requires creating a mesh structure in the given computational domain. Upon creation of such a mesh, the domain is represented by nodal points which are connected with each other through the created mesh. The numerical solution of Eqn. (8) is sought in those nodes. This mesh has been generated using the commercial package GAMBIT. The mesh is shown in **Fig. 22.**

7.3 Detail of the mesh structure

The CGWAVE model utilizes triangular mesh units in the computational domain. Due to the complexity in the shoreline geometry (as can be seen in **Fig.21**) which includes the proposed groyne, an unstructured mesh is desired. Hence a triangular unstructured mesh is generated in GAMBIT, mesh generation software. In such a mesh the nodal spacing is optimized so as to adapt to the nearby portion of the shoreline boundary. The outer semi circular periphery is modeled by 1265 nodes with a spacing of 5 m and the inner shoreline is modeled by nodes with a spacing of 5 m. Then an unstructured mesh is created with an average spacing of 5m inside the domain. This leads to a total number of 147455 nodes with 393820 numbers of triangular elements.

7.4 Results and discussion

A total number of three wave directions have been simulated in order to investigate the wave tranquility inside the proposed breakwater. The wave directions are chosen such that these represent an annual year. The wave period of the computations is given as 8s to observe the wave climate. The incident wave angle is varied to simulate different wave directional scenarios.

The wave climates representing typical wave directions are presented. **Fig.23** to **Fig.27** present the wave phase diagram and the wave height distribution for the three cases

representing the wave crest propagation for the wave approach angles 45^{0} , 90^{0}, 135^{0}, 155^{0} and 180^{0} respectively.

8.0 RECOMMENDATIONS

The optimized revised harbour layout for the fishing harbour at Thiruvottriyur kuppam is given in Plate 1 by satisfying the tranquility requirements inside the breakwaters and, the simulation from the shoreline change study indicates the erosion on the north. However, the series of groynes on the north would mitigate the erosion. Hence, the Proposed revised layout is recommended.

Prof. S.A. Sannasiraj   **Prof. V. Sundar**

9.0 REFERENCES

1. **Berkhoff**(1972)Computation of combined Refraction and –Diffraction.

2. **CERC** (1984) Shore Protection Manual. Coastal Engineering Research Centre, US.

3. **Coastal Engineering Manual**, 2006. Part VI

4. **Goda,Y.** (1985) Random seas and design of maritime structures.

5. **Kressener**(1928)Tests with scale models to determine the effect of currents and breakers upon a sandy beach, and the advantageous installation of groins.

6. **Owen and Allsop** (1983), Hydraulic modelling of rubble mound breakwaters, Proceedings of the conference organized by Institute of Civil Engineers, London.

7. **Sundar, V.** (2005) Behaviour of groins. Fifth international symposium on wave measurement and analysis, WAVES 2005, Madrid, Spain, 3-7 July.

8. **US Army Engineer District, Willington (1973)** Hurricane-Wave protection-Beach-Erosion control Brunswick country, N.C., Beach projects, Yaupon beach and long beach segments.

9. **Komar, P.D.(1976a),** *Beach process and sedimentation, Prentice –Hall Englewood Cliffs,* N.J., 429p.

10. **Komar,P.D.(1976b),** *Longshore currents and sand transport on ocean Eng. III,* ASCE,333-354.
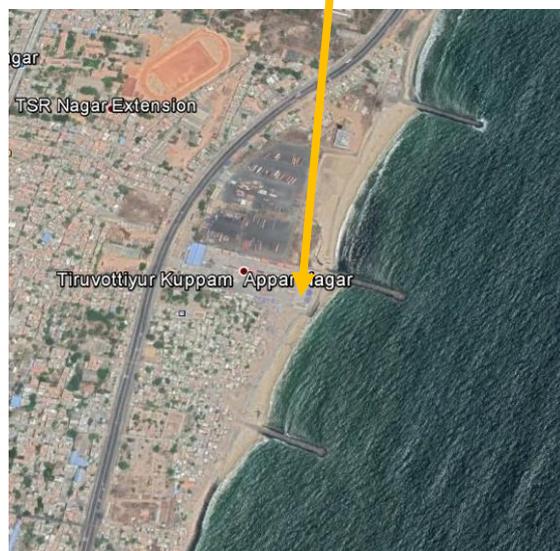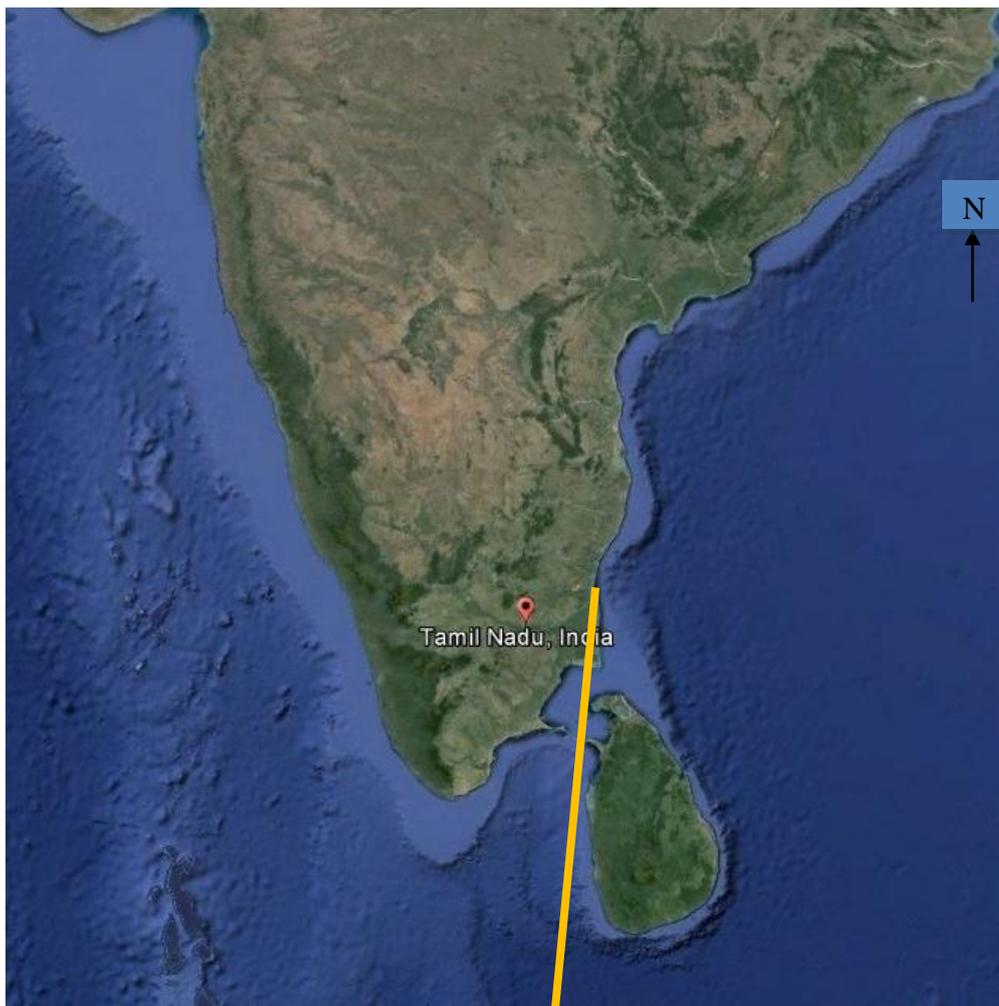
Fig.1 Aerial view of Thiruvottriyur Kuppam
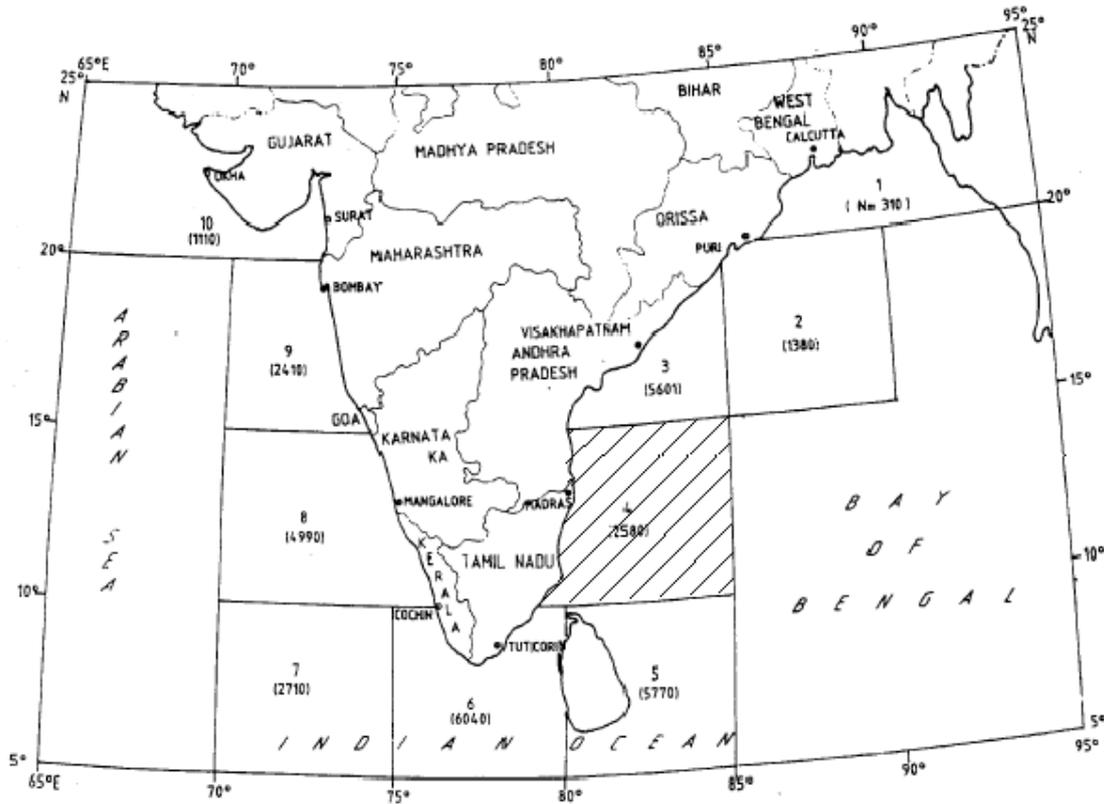
Fig.2 Grid on wave atlas for study area
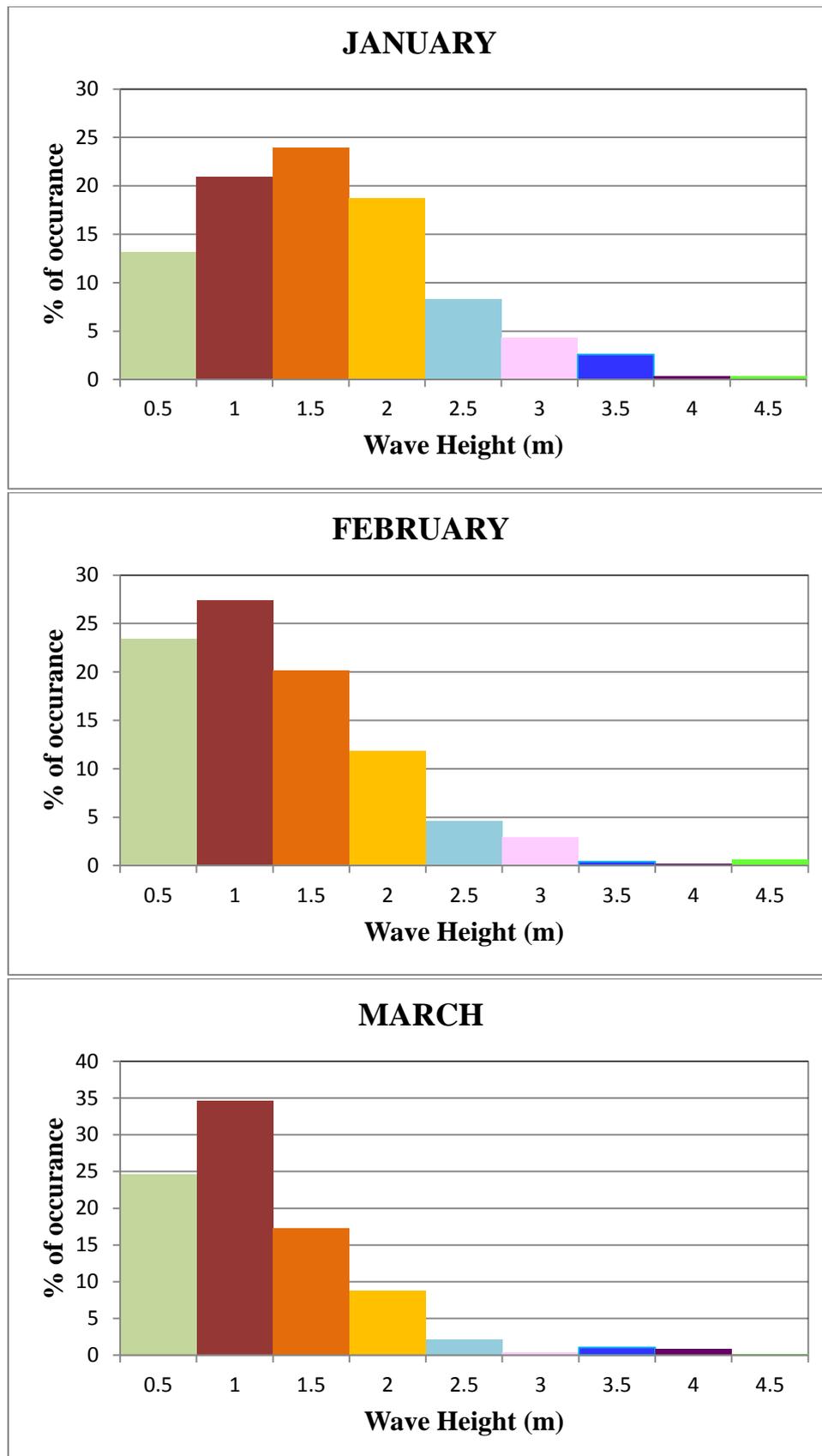
Fig.3 Monthly distribution of wave heights (Jan-Mar)
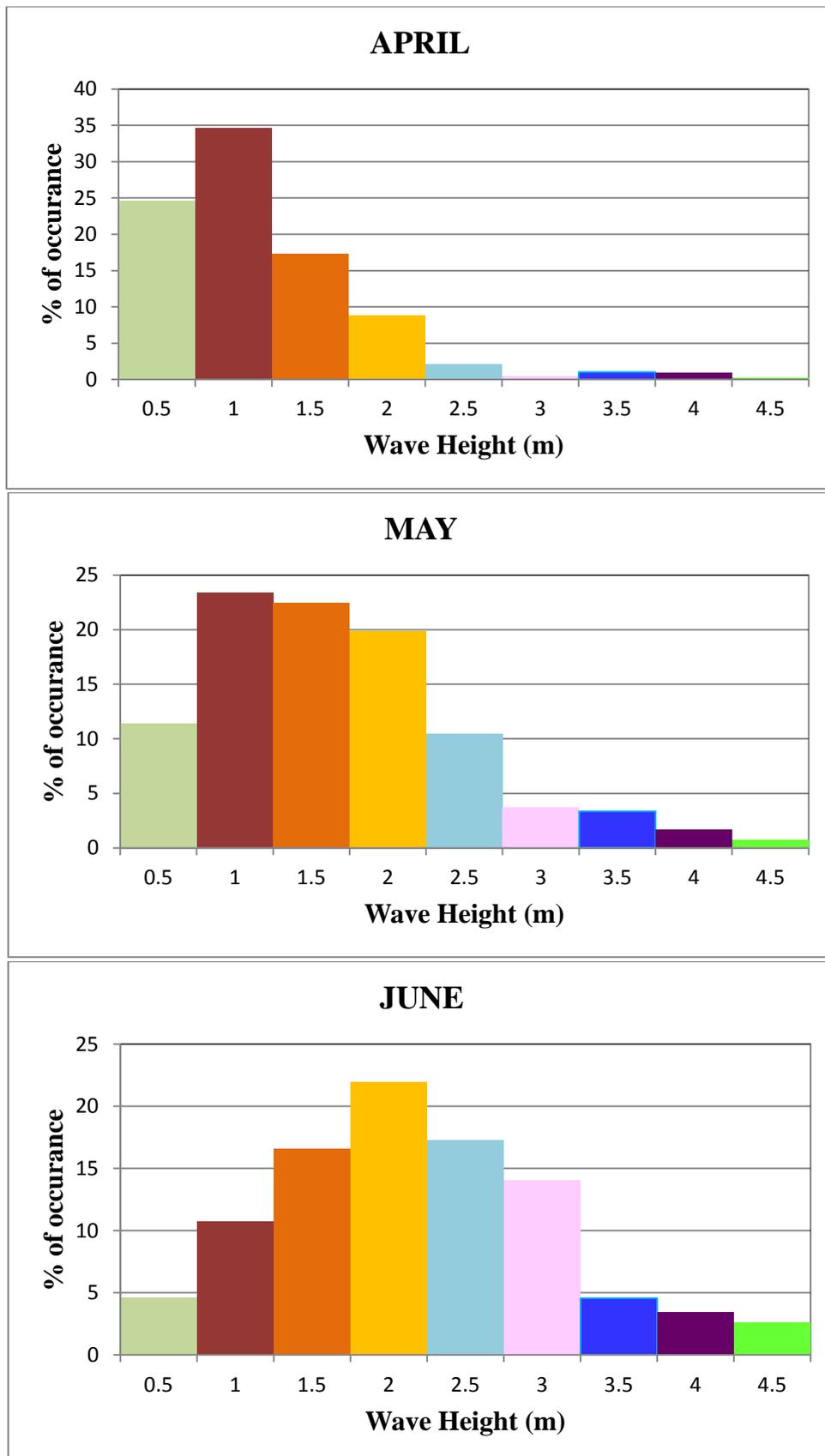
Fig.4 Monthly distribution of wave heights (Apr – June)
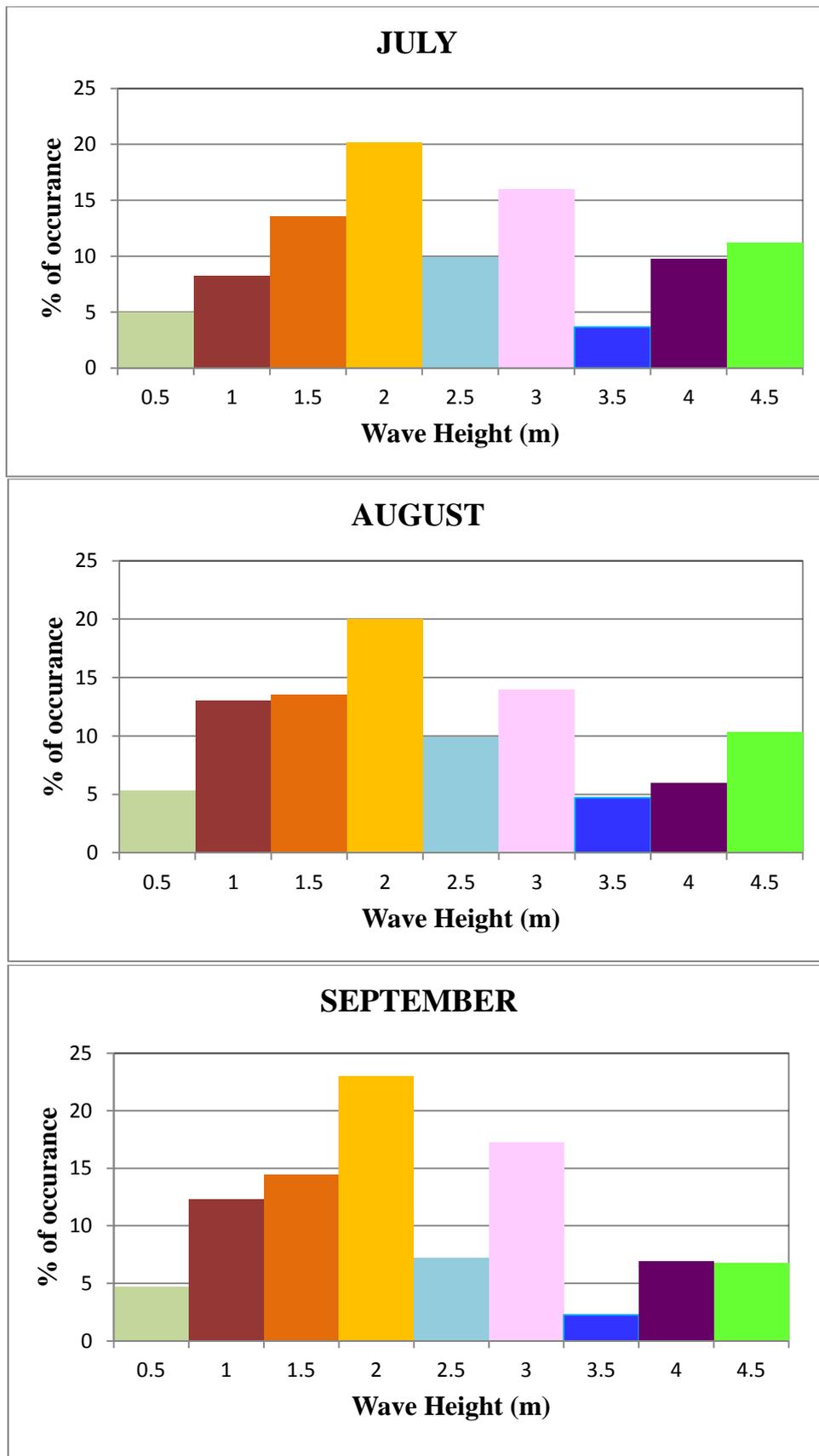
Fig.5 Monthly distribution of wave heights (July – Sep)
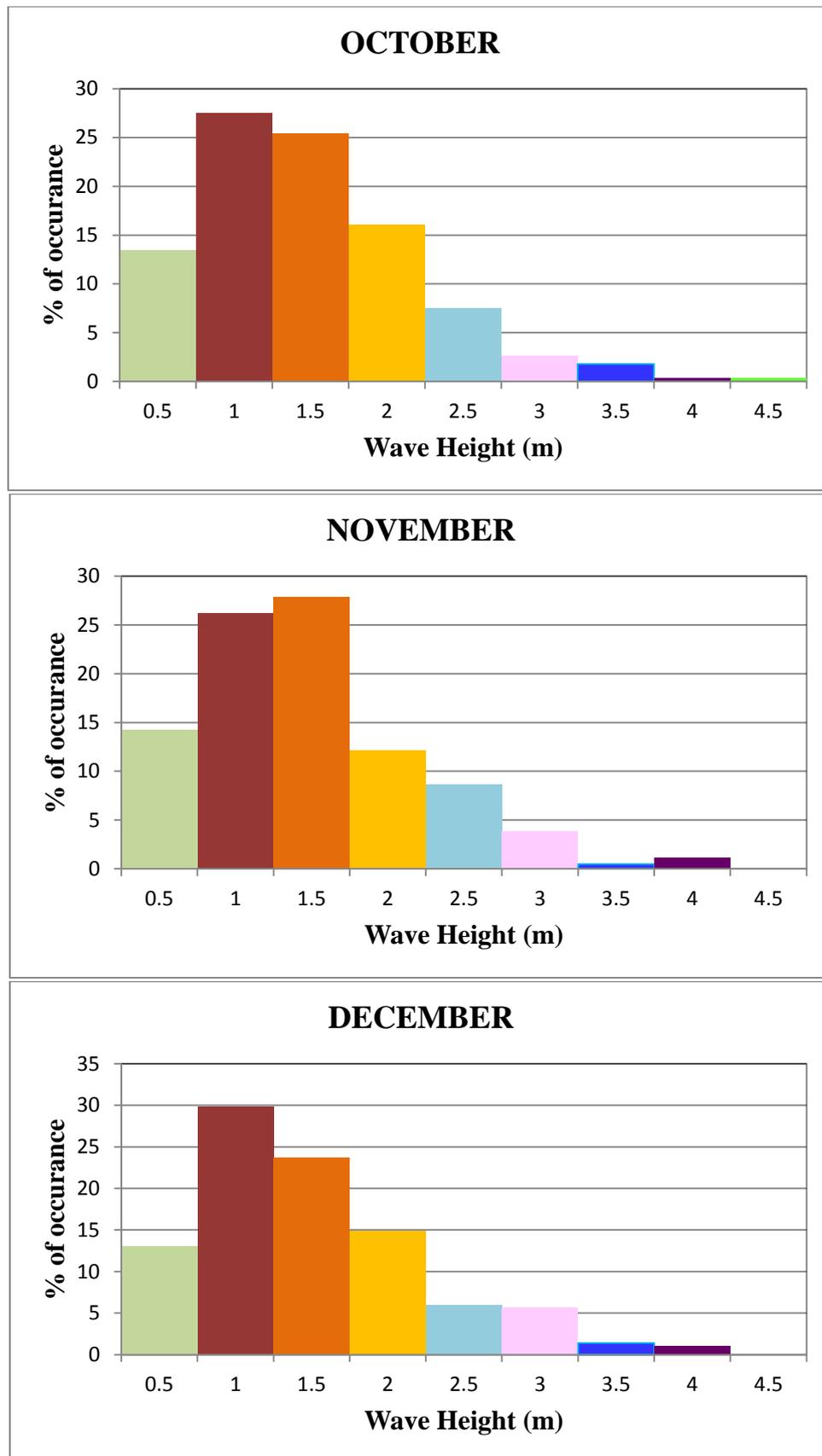
Fig.6 Monthly distribution of wave heights (Oct – Dec)
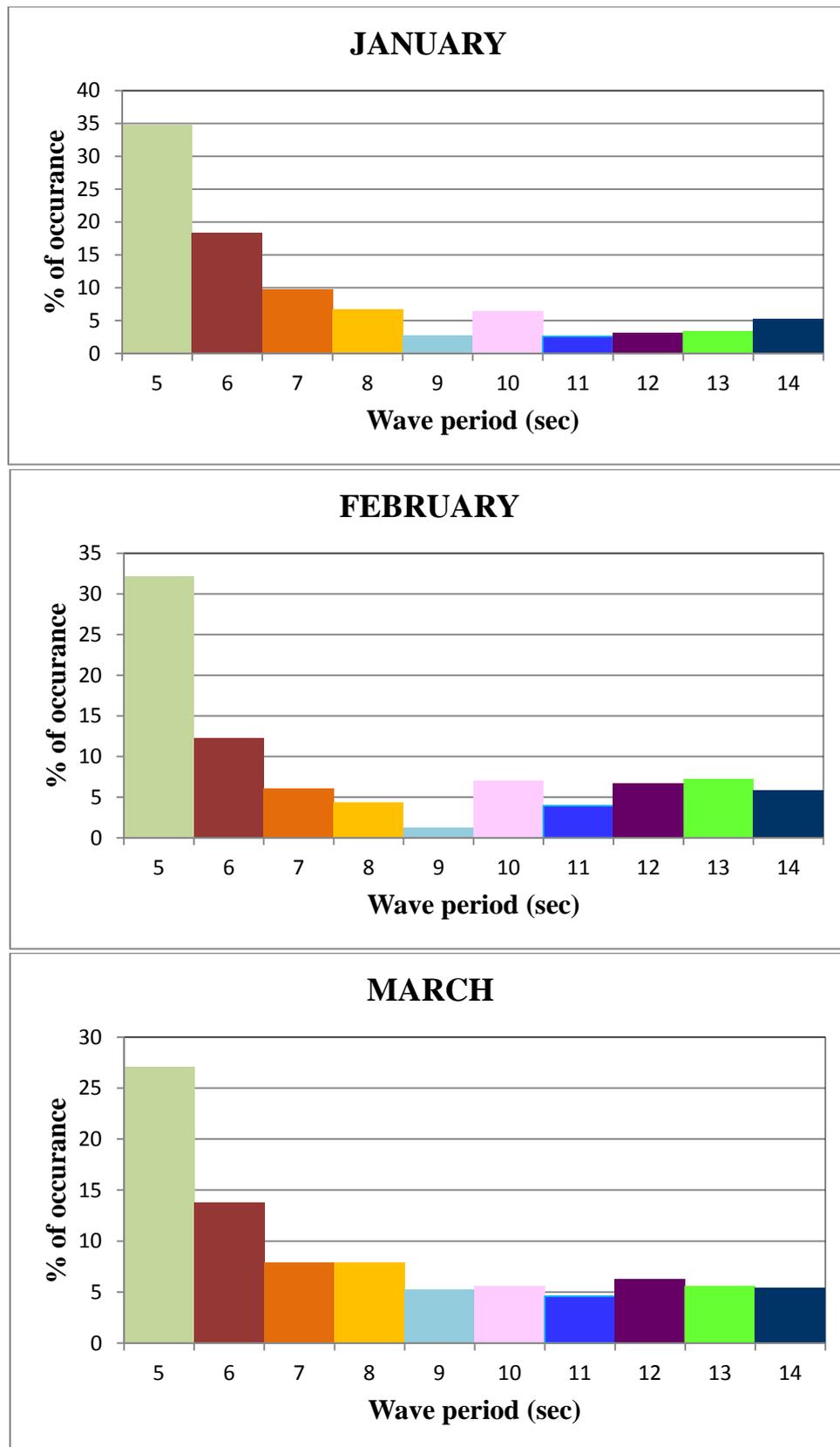
Fig.7 Monthly distribution of wave periods (Jan- Mar)
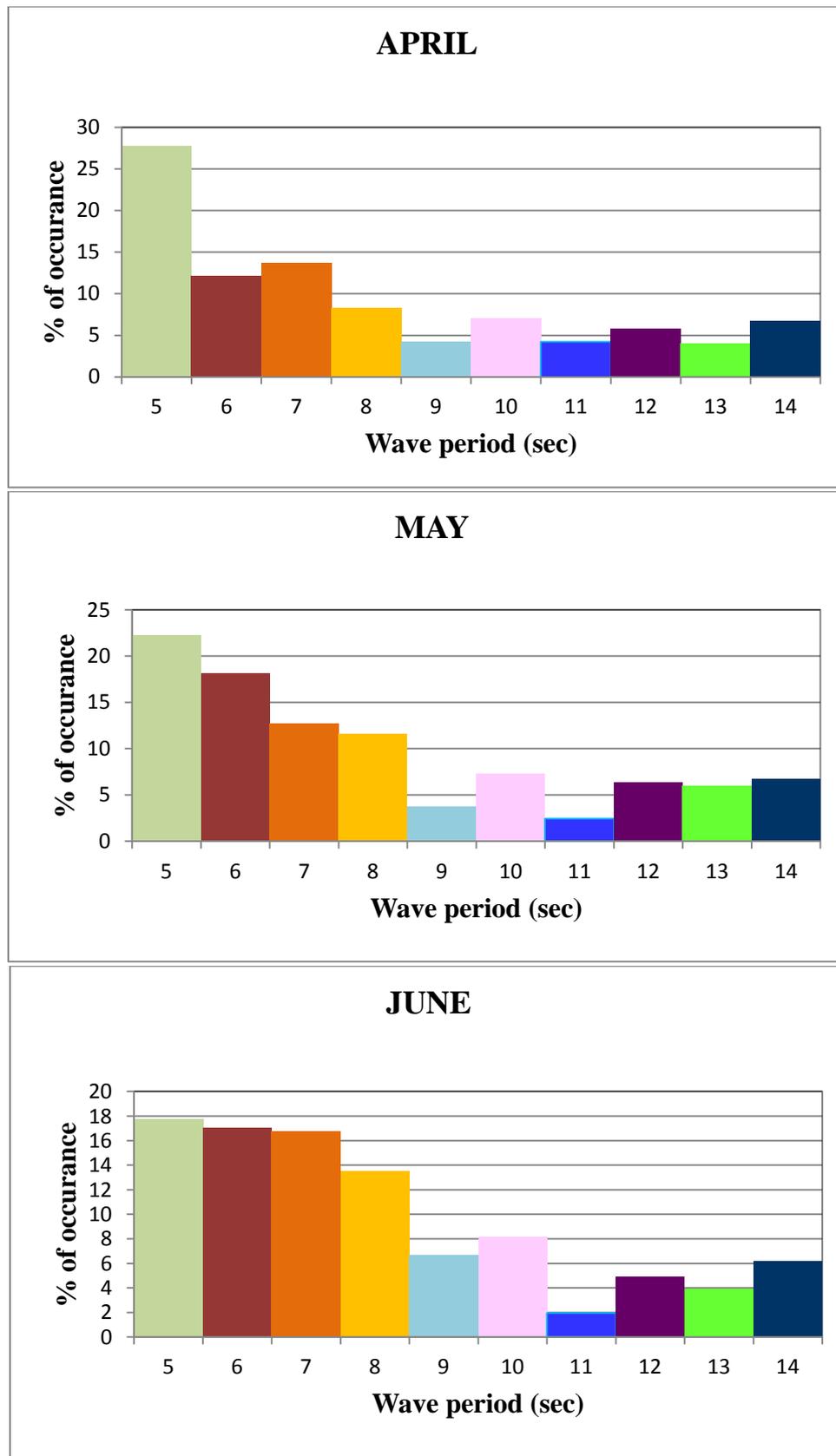
Fig.8 Monthly distribution of wave periods (Apr- June)
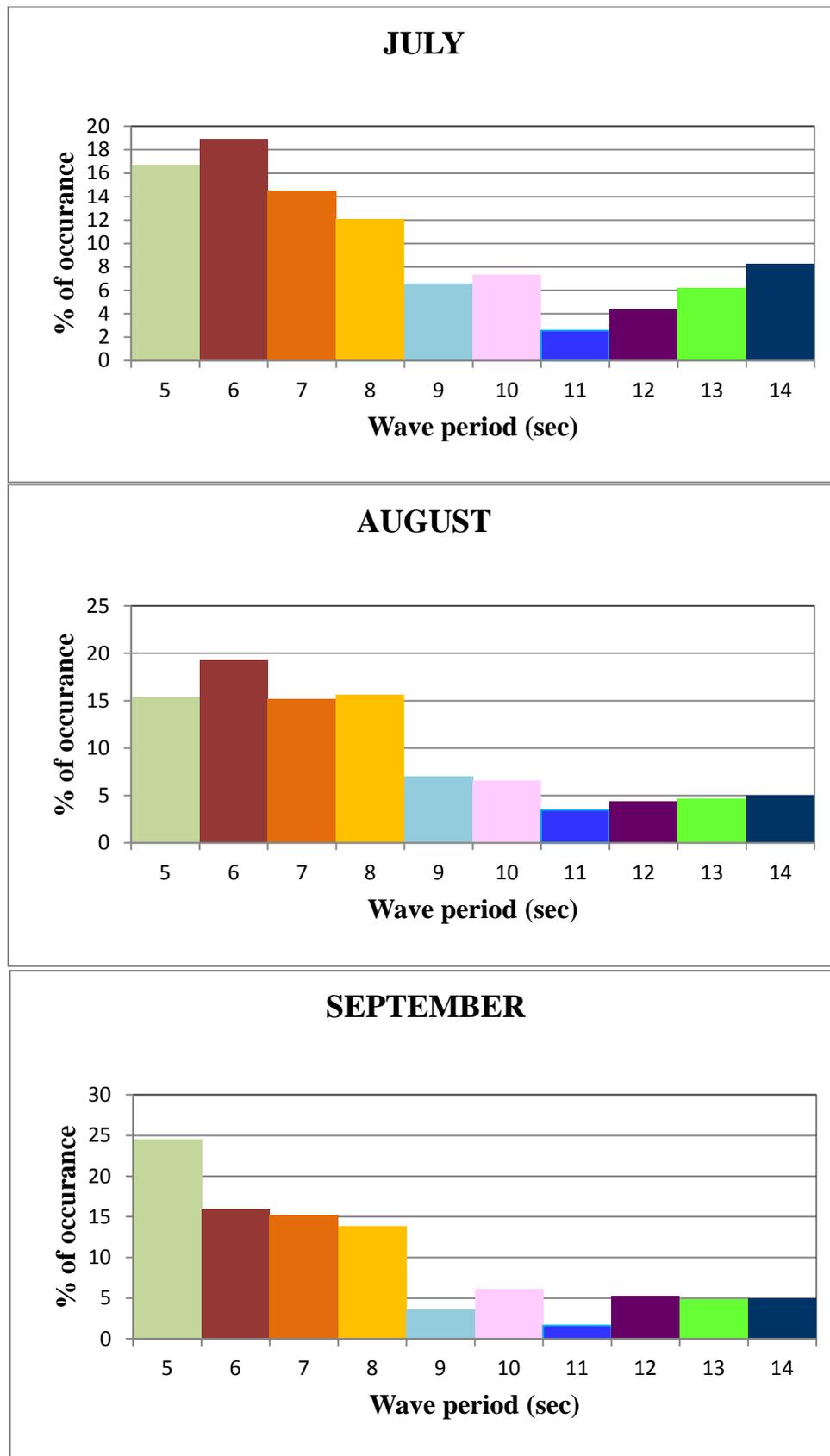
Fig.9 Monthly distribution of wave periods (July – Sep)
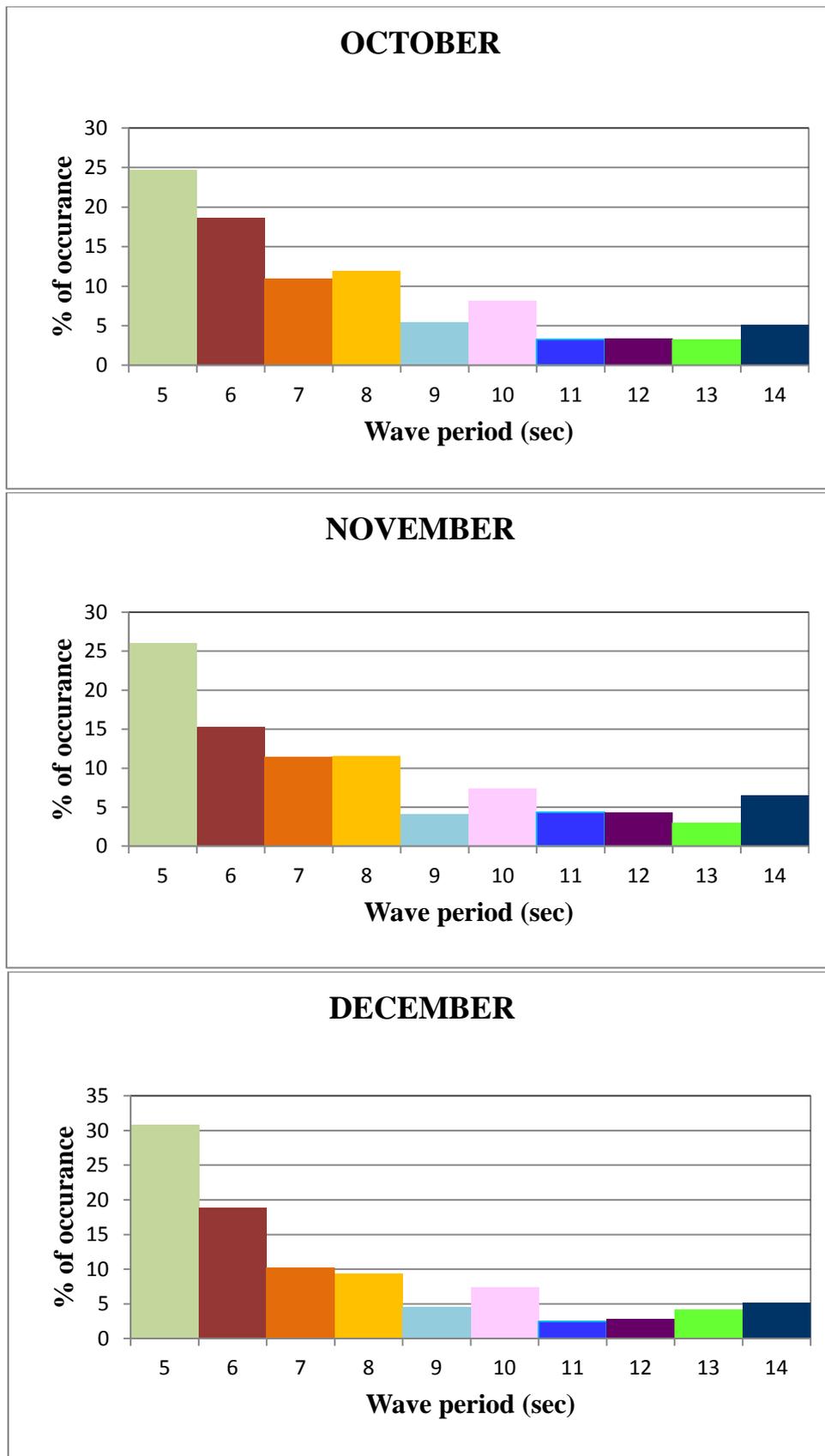
Fig.10 Monthly distribution of wave periods (Oct – Dec)
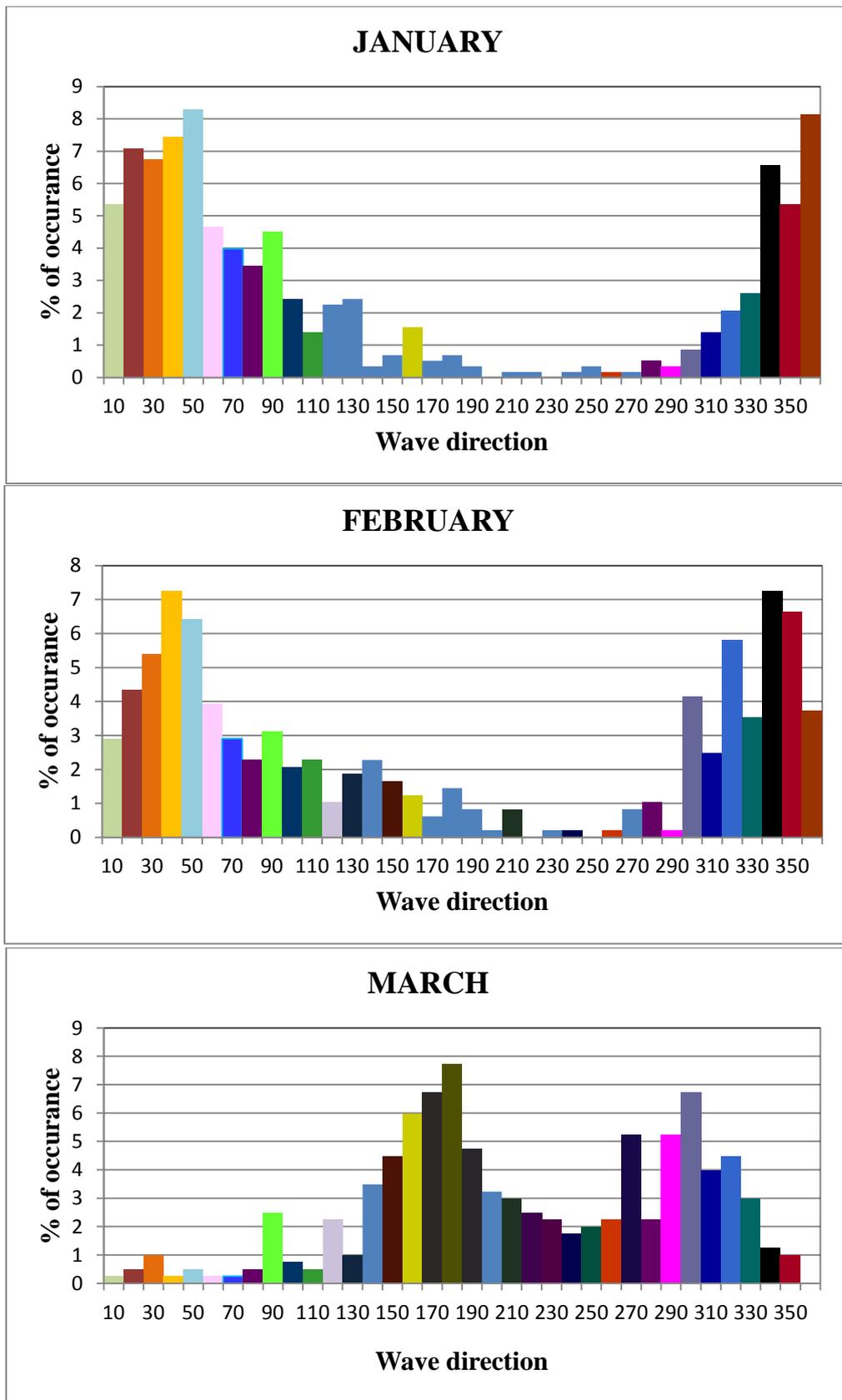
Fig.11 Monthly distribution of wave directions (Jan – Mar)
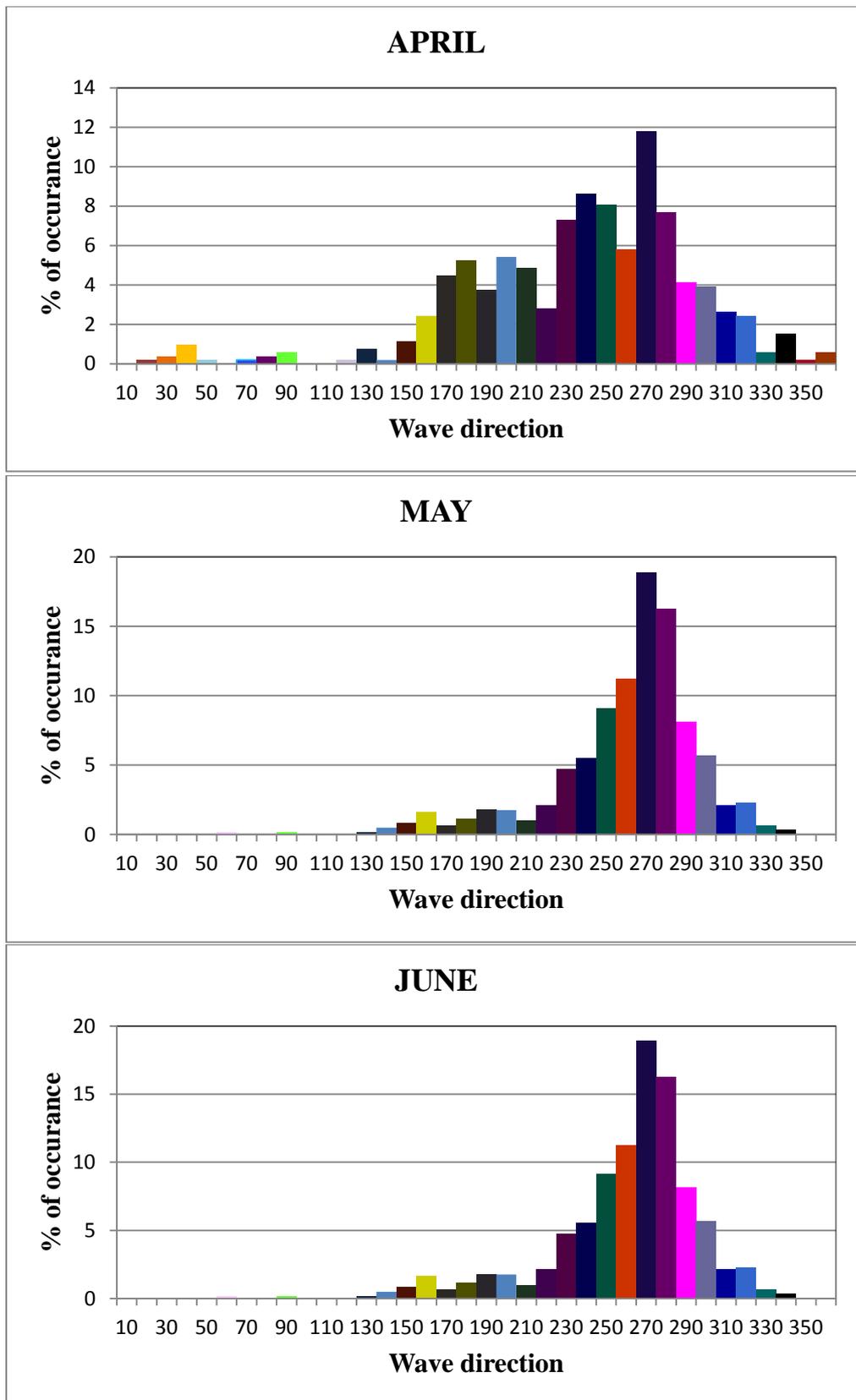
Fig.12 Monthly distribution of wave directions (Apr – June)

JULY

AUGUST

SEPTEMBER
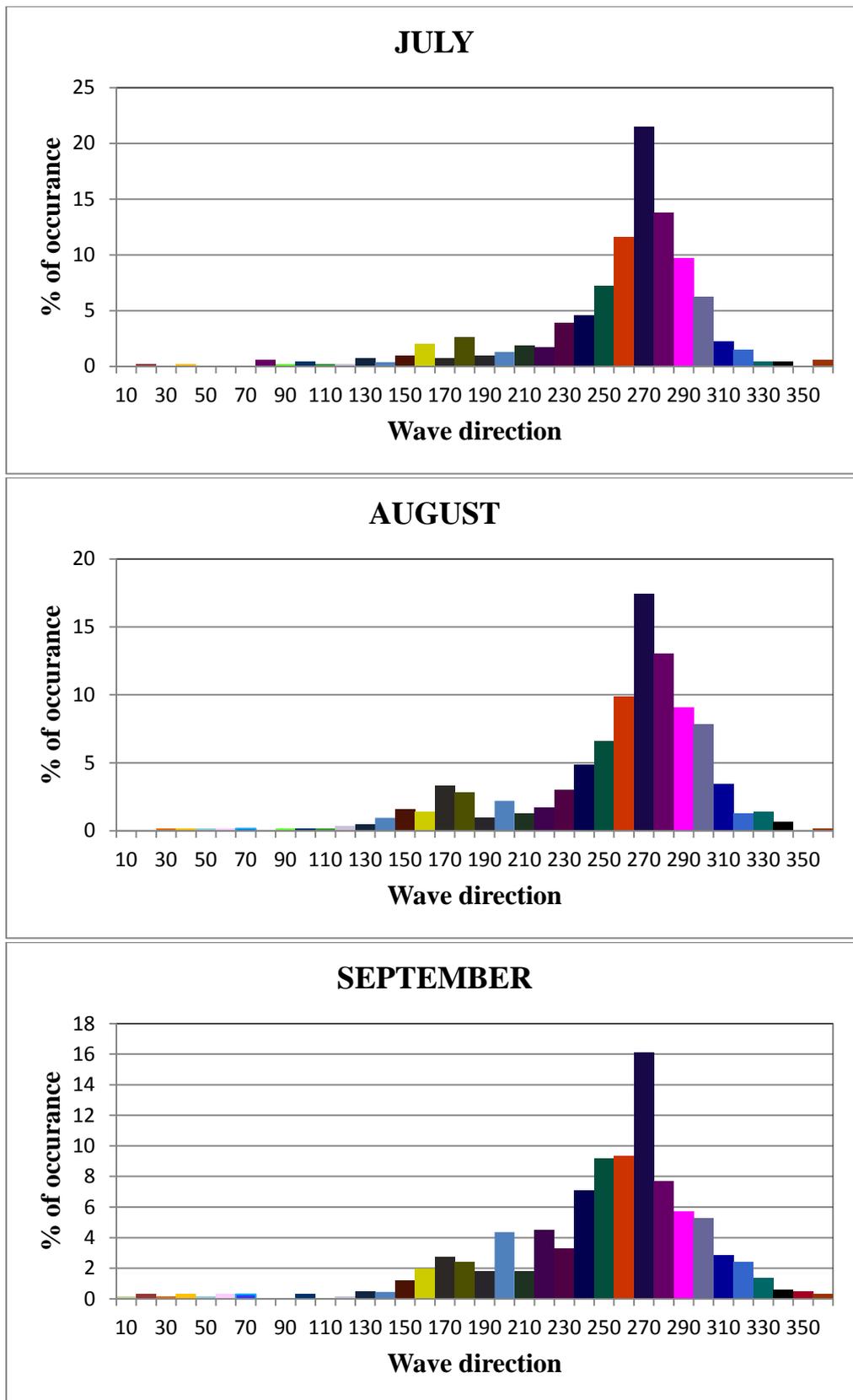
Fig.13 Monthly distribution of wave directions (July – Sep)
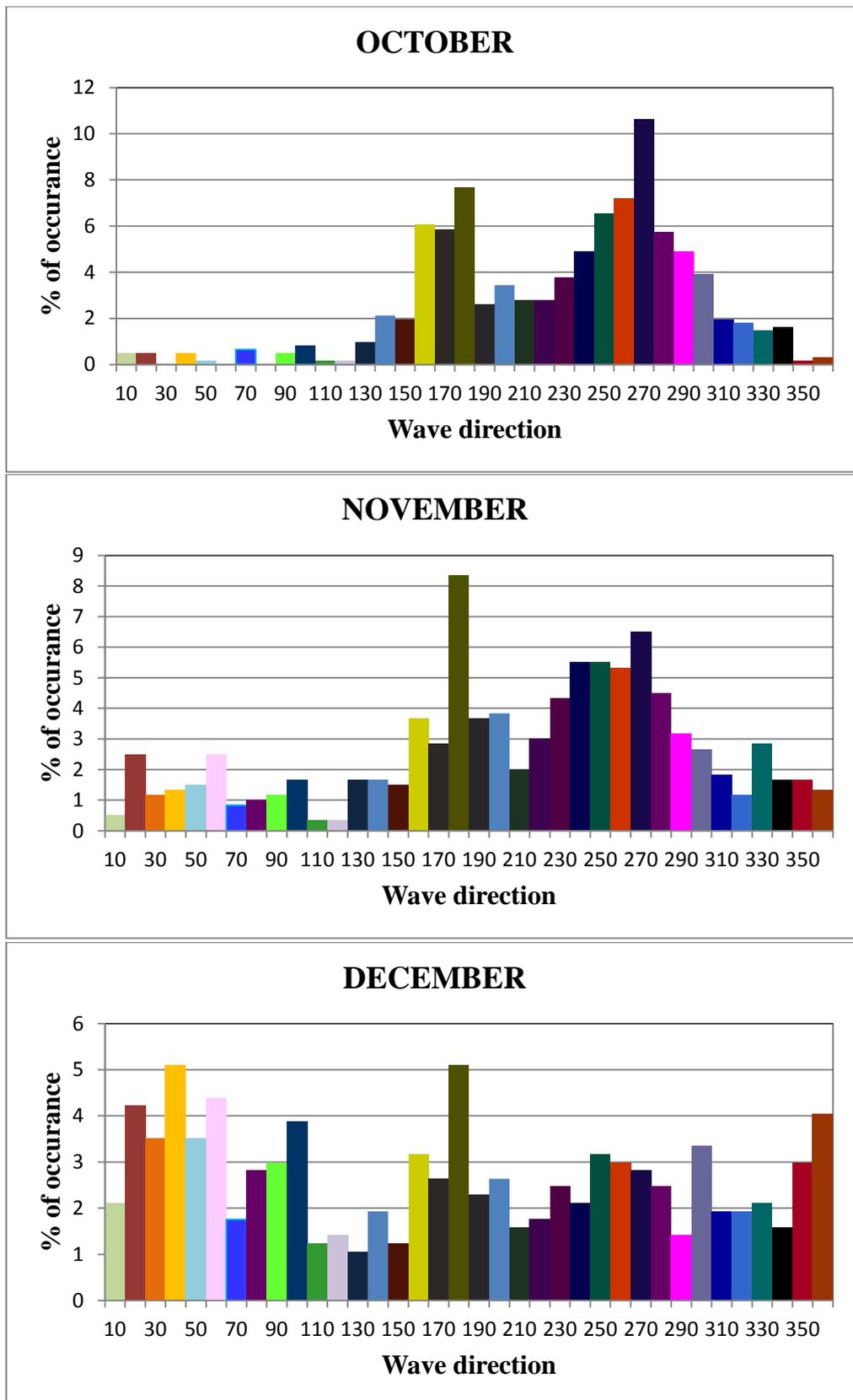
Fig.14 Monthly distribution of wave directions (Oct – Dec)
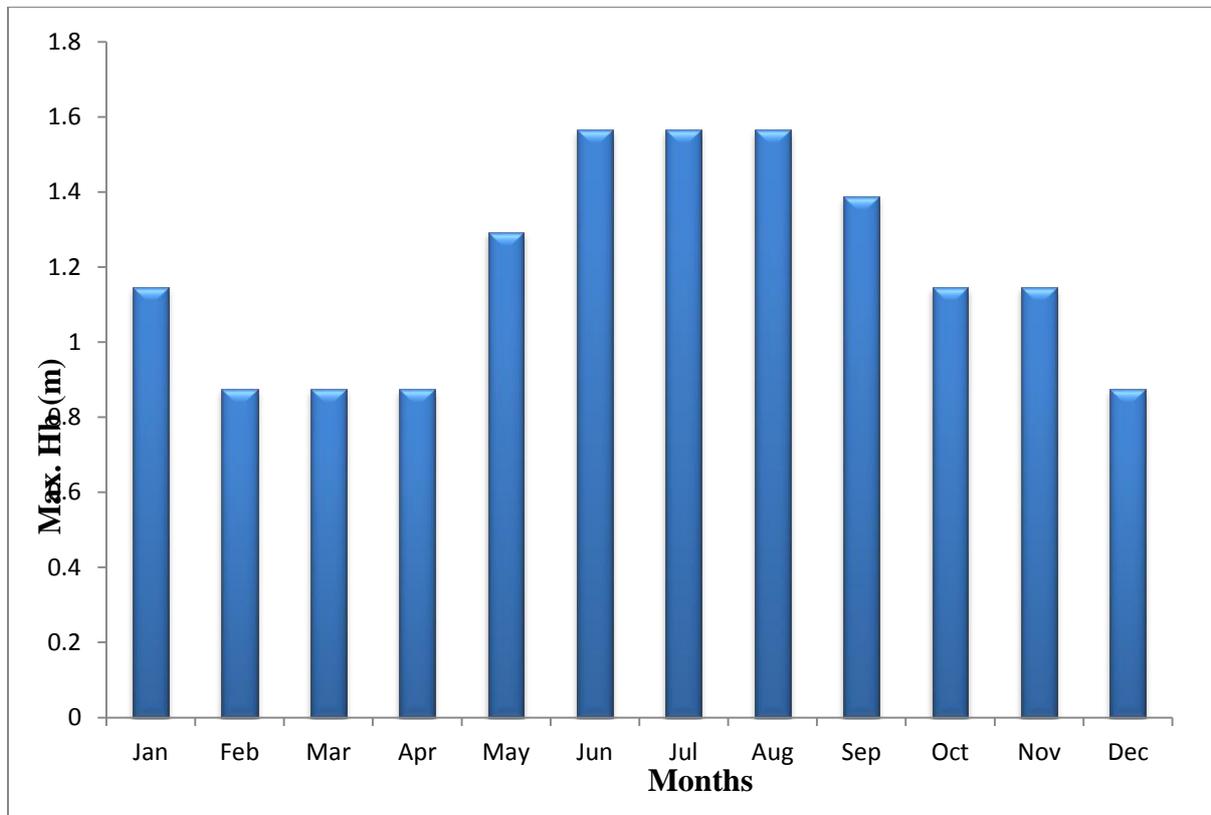
Fig.15(a) Mean Breaker Height for all months
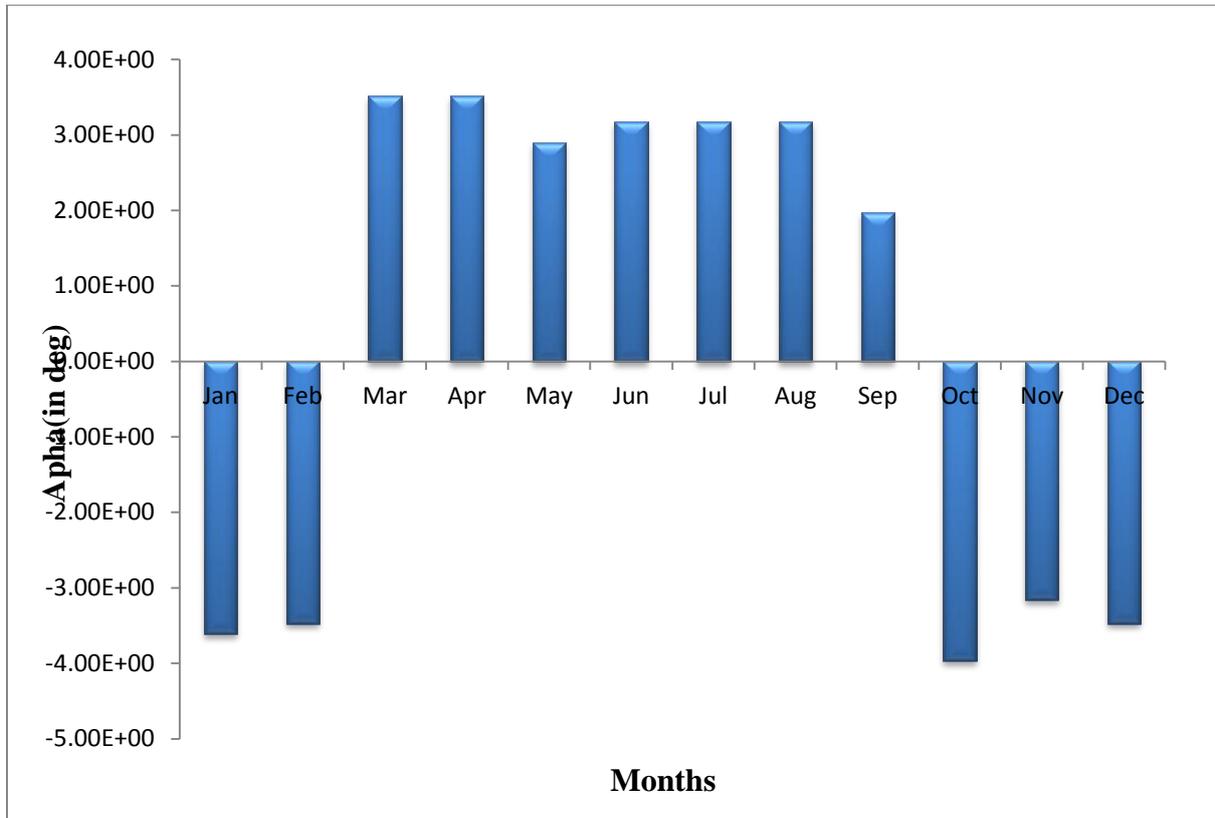
Fig.15(b) Mean Breaker Angle for all months
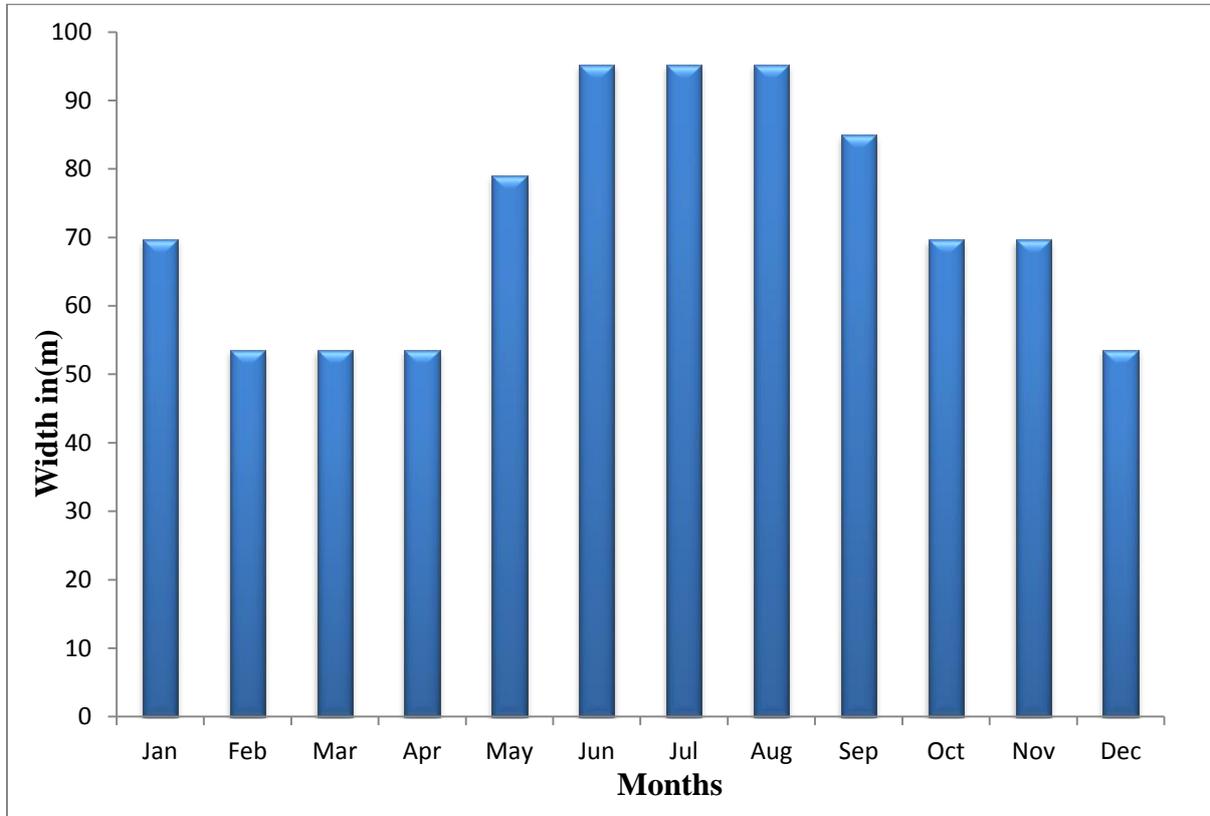
Fig.15(c) Mean Surf Zone Width for all months

Fig.16 Long shore sediment transport rate

Q1, Q2 = Longshore sediment transport rate at grid point
y1, y2 = Shoreline co-ordinate at mid point of grid
q1, q2 = Nourishment quantity at mid point of grid
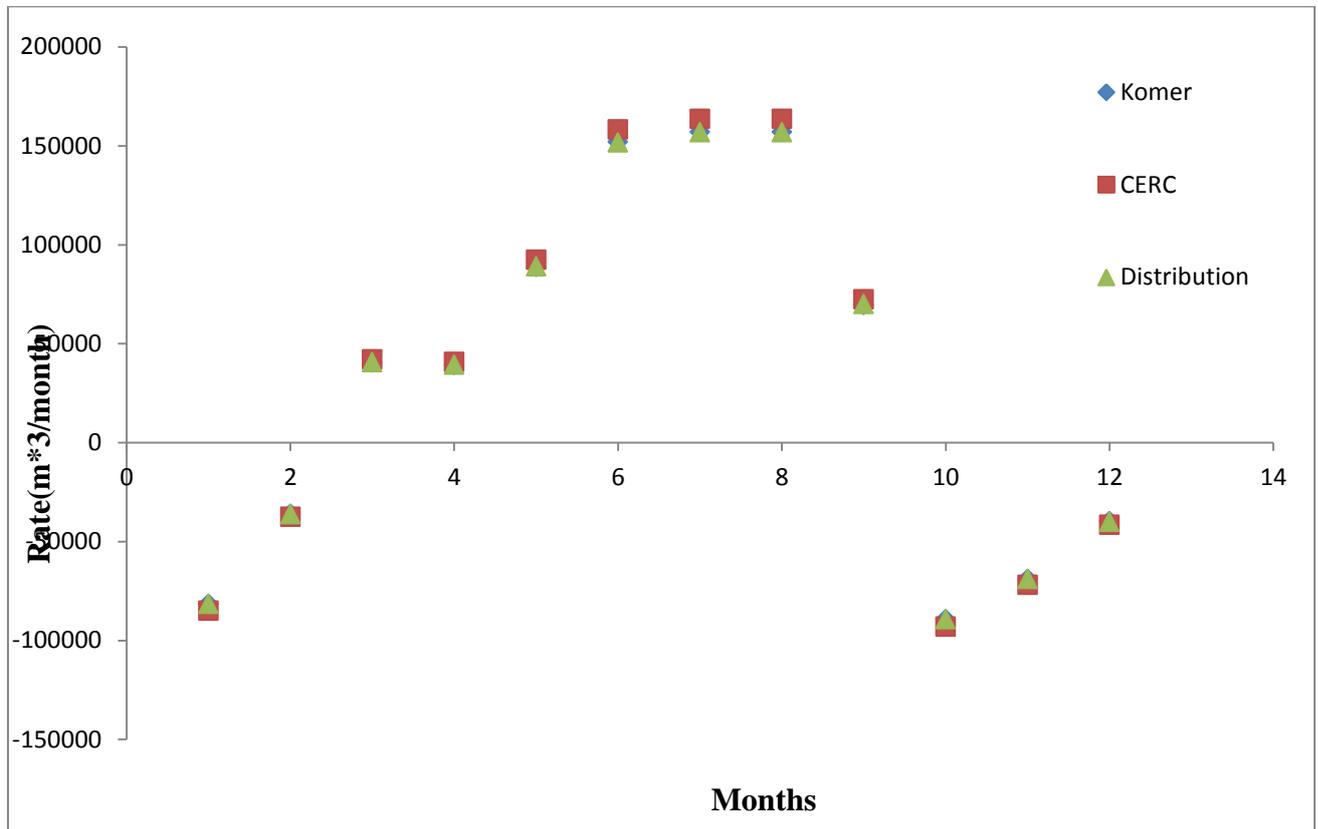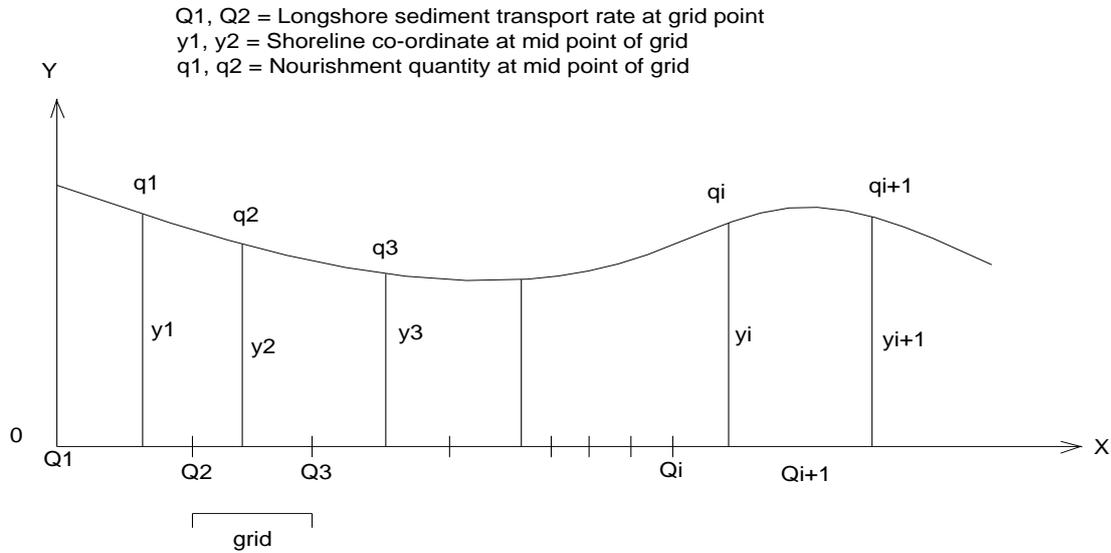
Fig.17 Schematic diagram for finite difference scheme
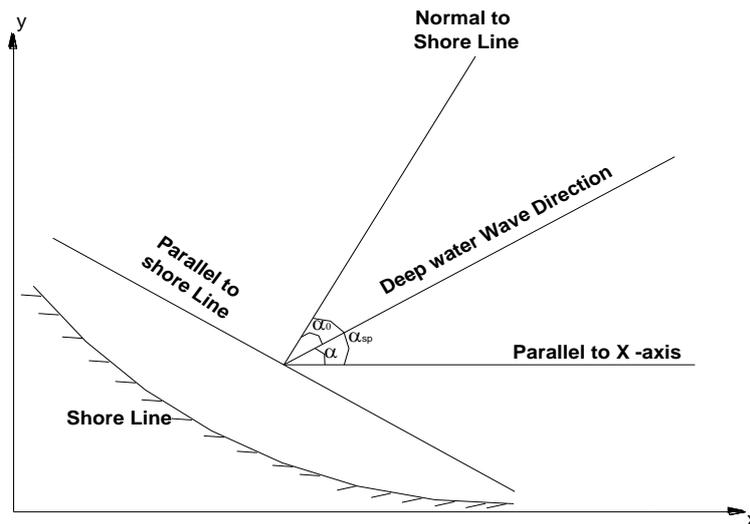
Fig.18 Definition sketch of angles considered
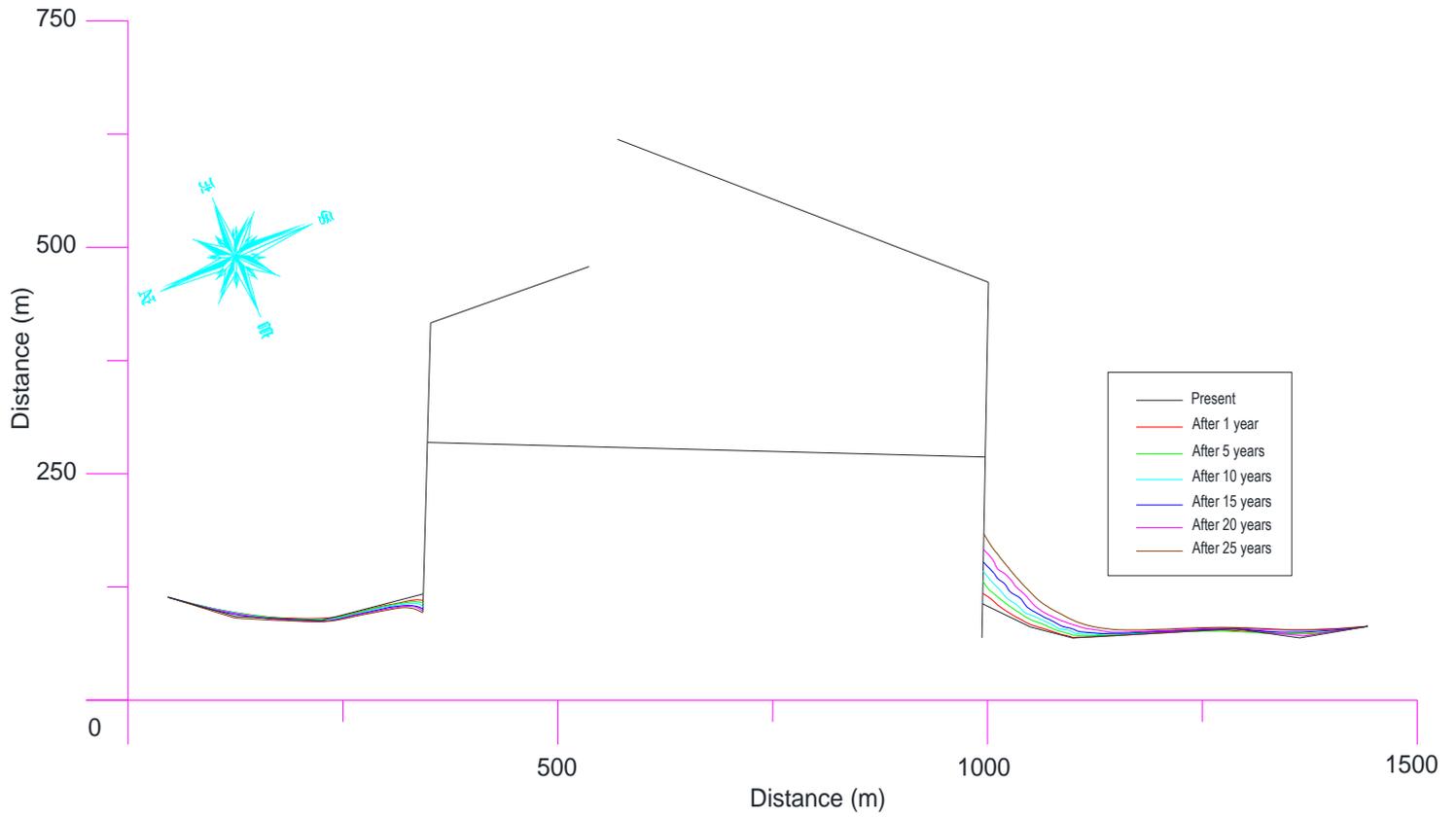
Fig.19 Shoreline evolution
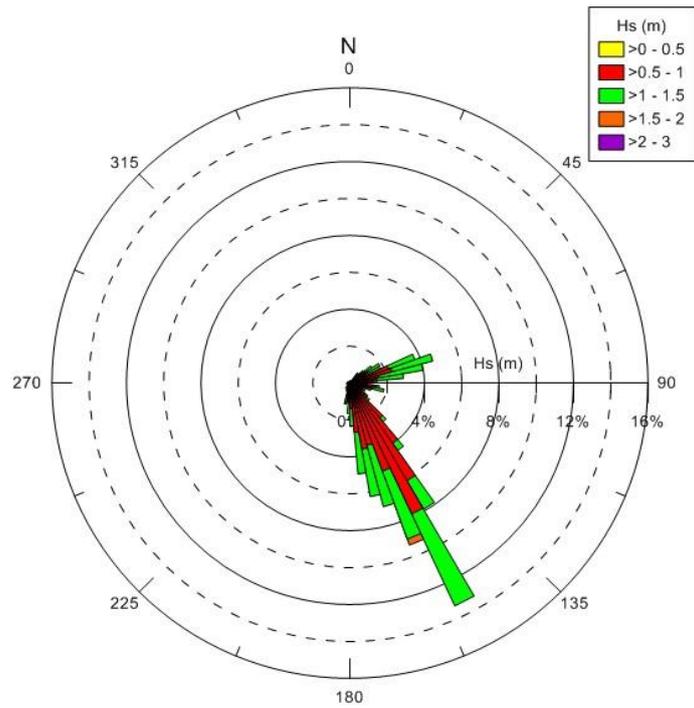
Fig.20 Wave rose diagram representing the significant wave height (m) along the particular direction for an annual year
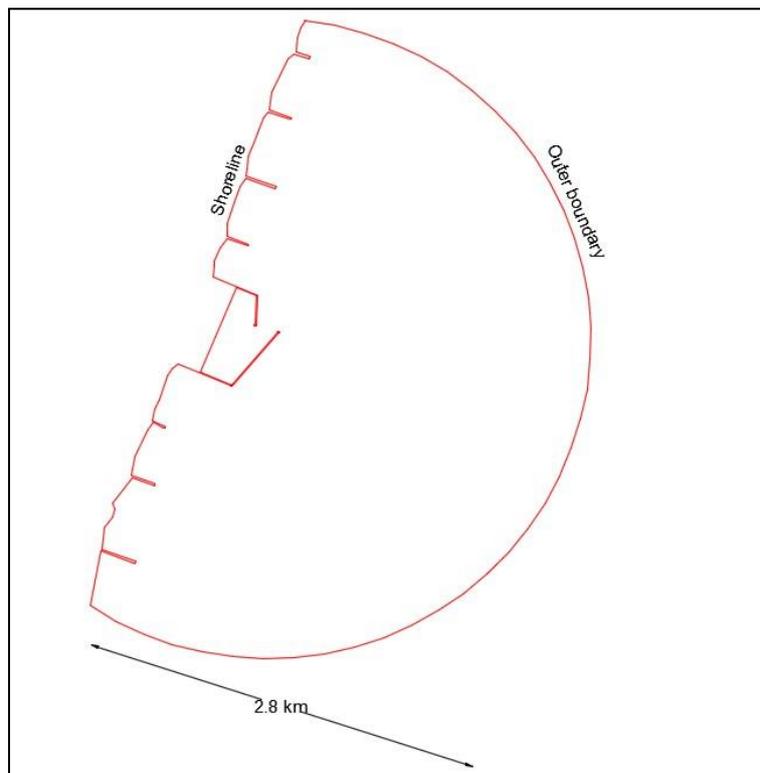
Fig.21 Computational domain for tranquility studies for Thiruvottriyur Kuppam
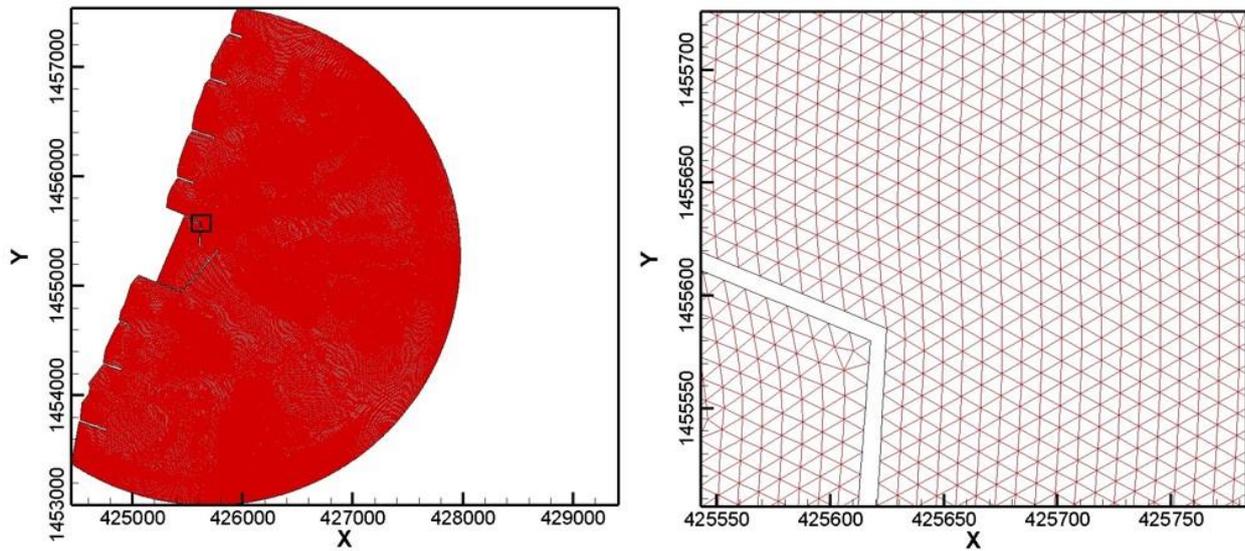
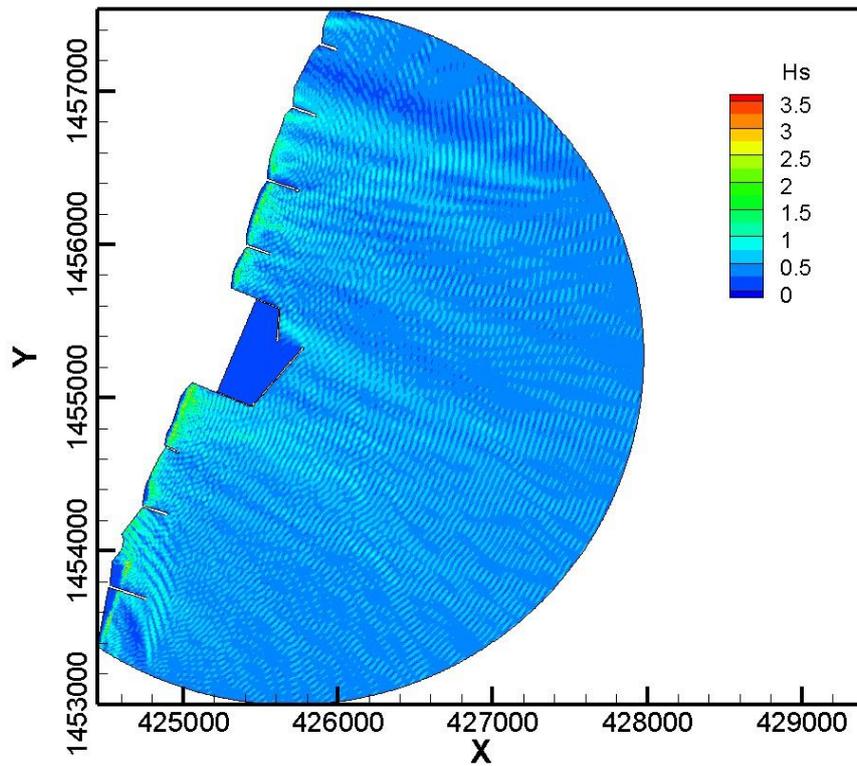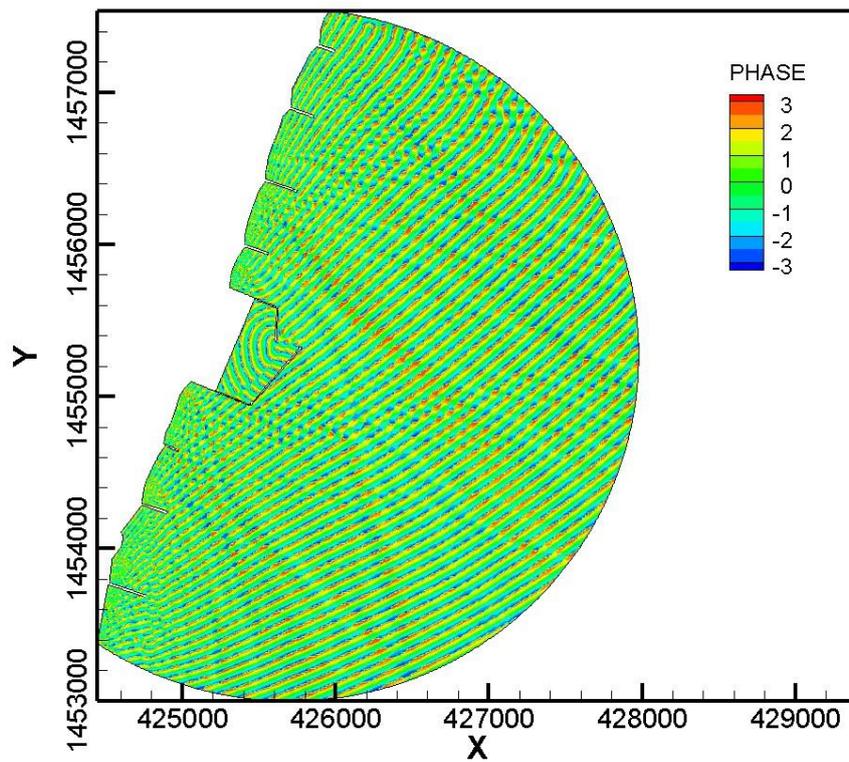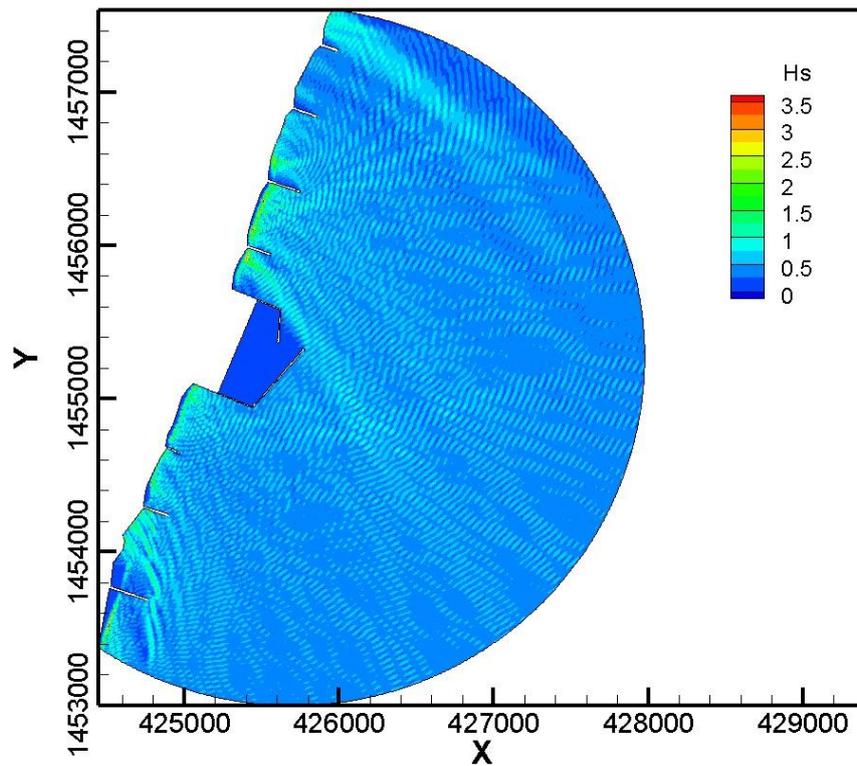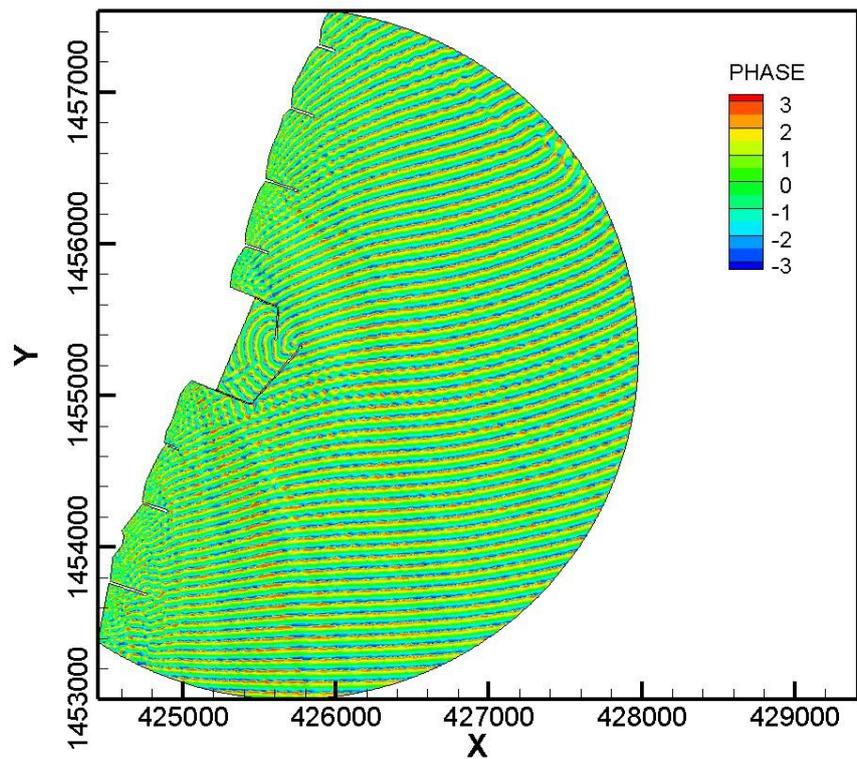**Fig.22 Mesh Structure adopted for the wave propagation modeling**
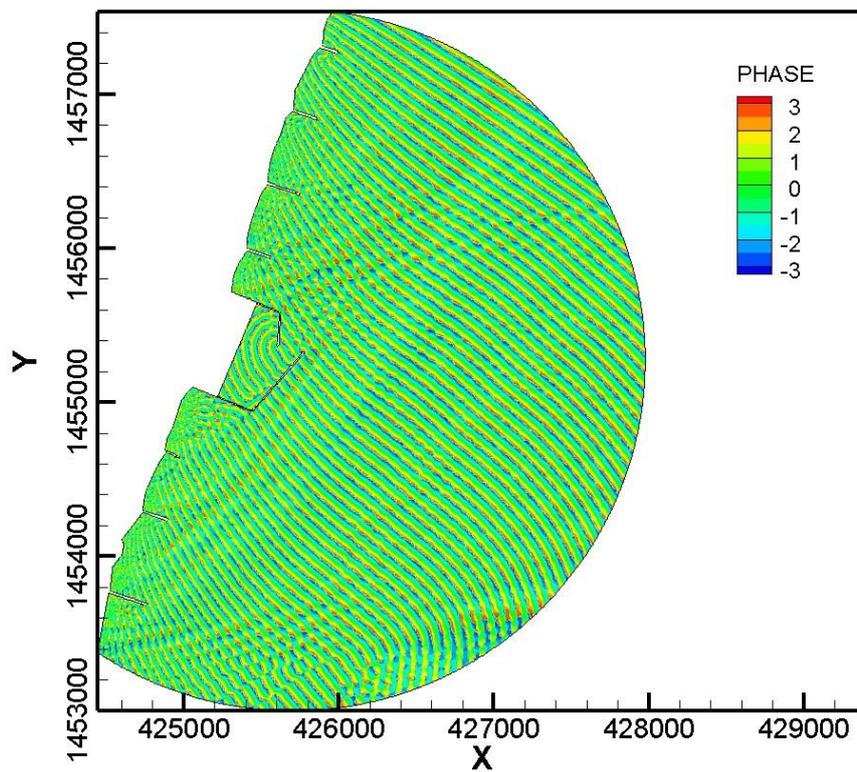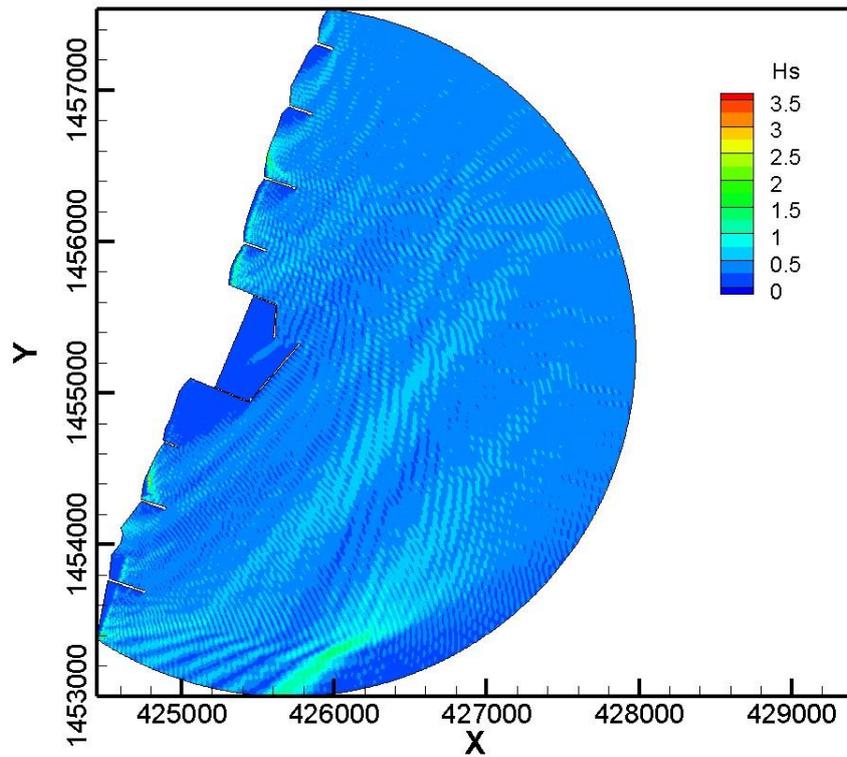
Fig.23 Phase distributions and Wave height distribution for the wave approach angle from 45^0
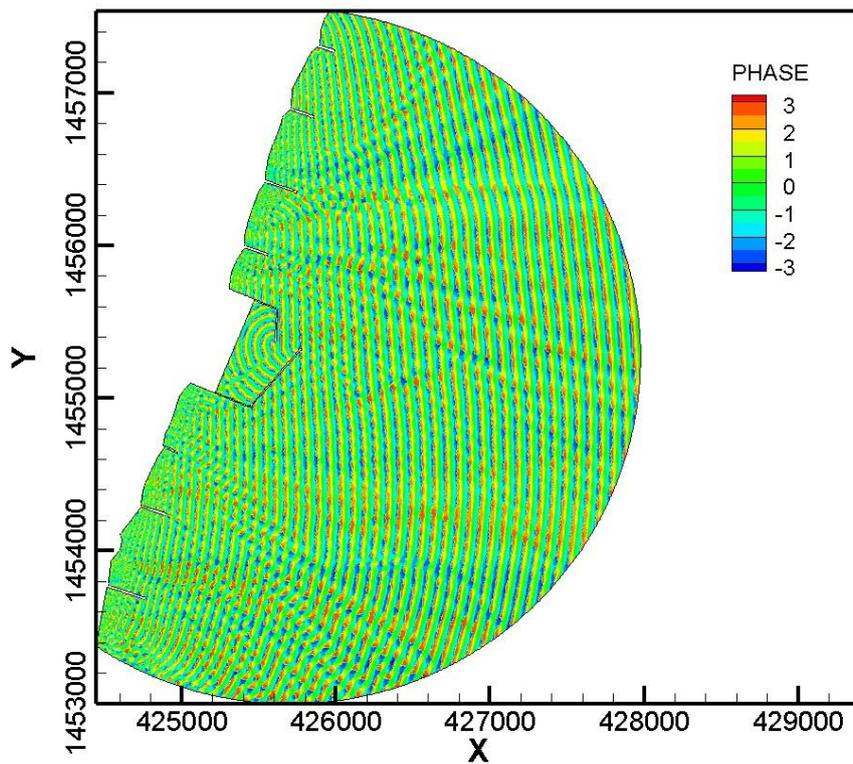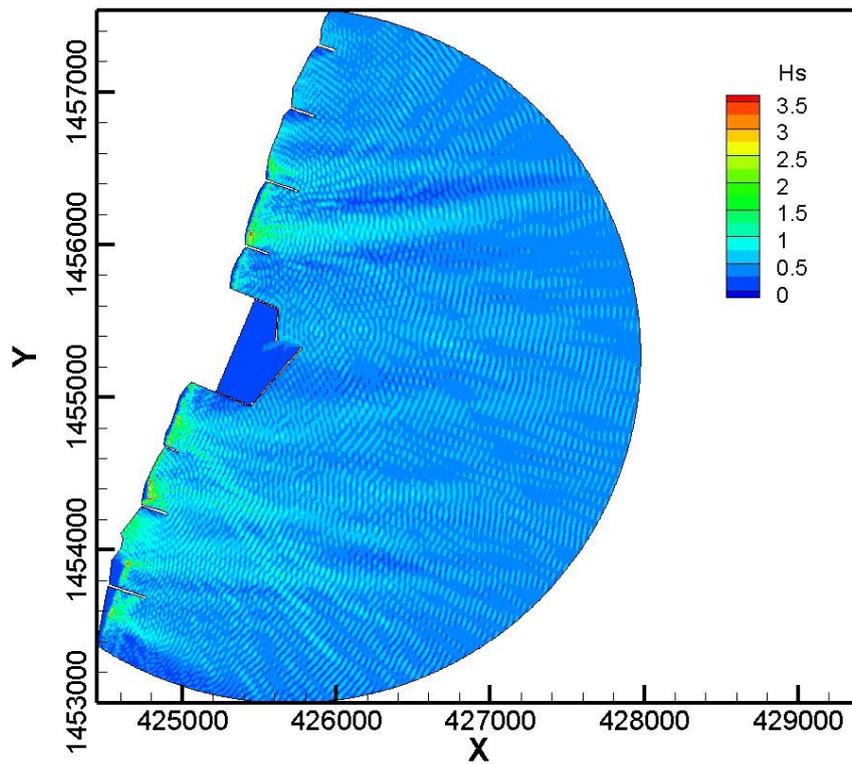
Fig.24 Phase distributions and Wave height distribution for the wave approach angle from 90^0
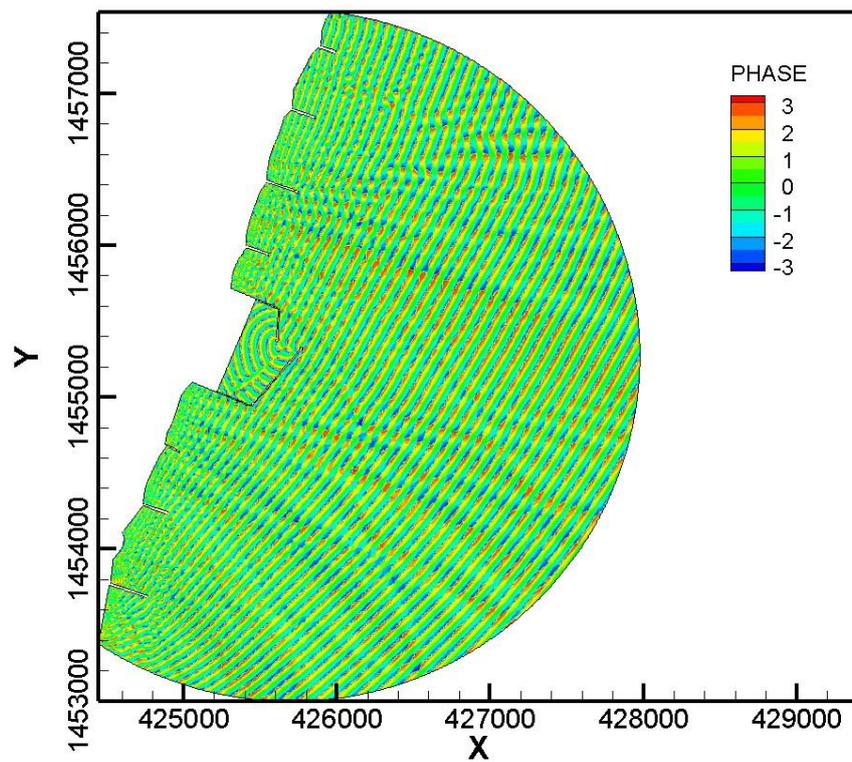
Fig.25 Phase distributions and Wave height distribution for the wave approach angle from 135^0

Fig.26 Phase distributions and Wave height distribution for the wave approach angle from 155^0
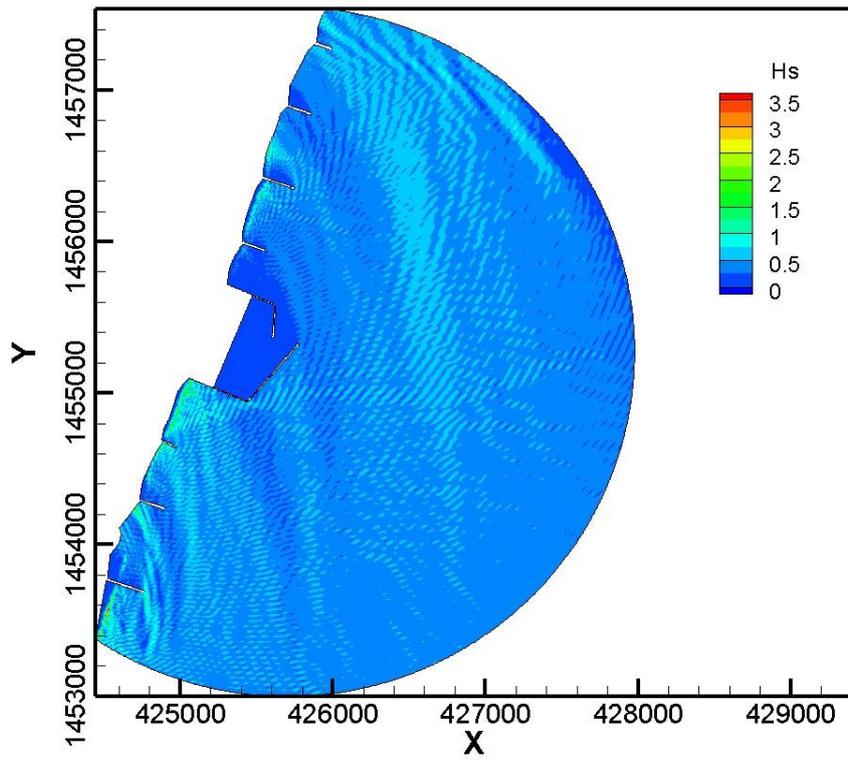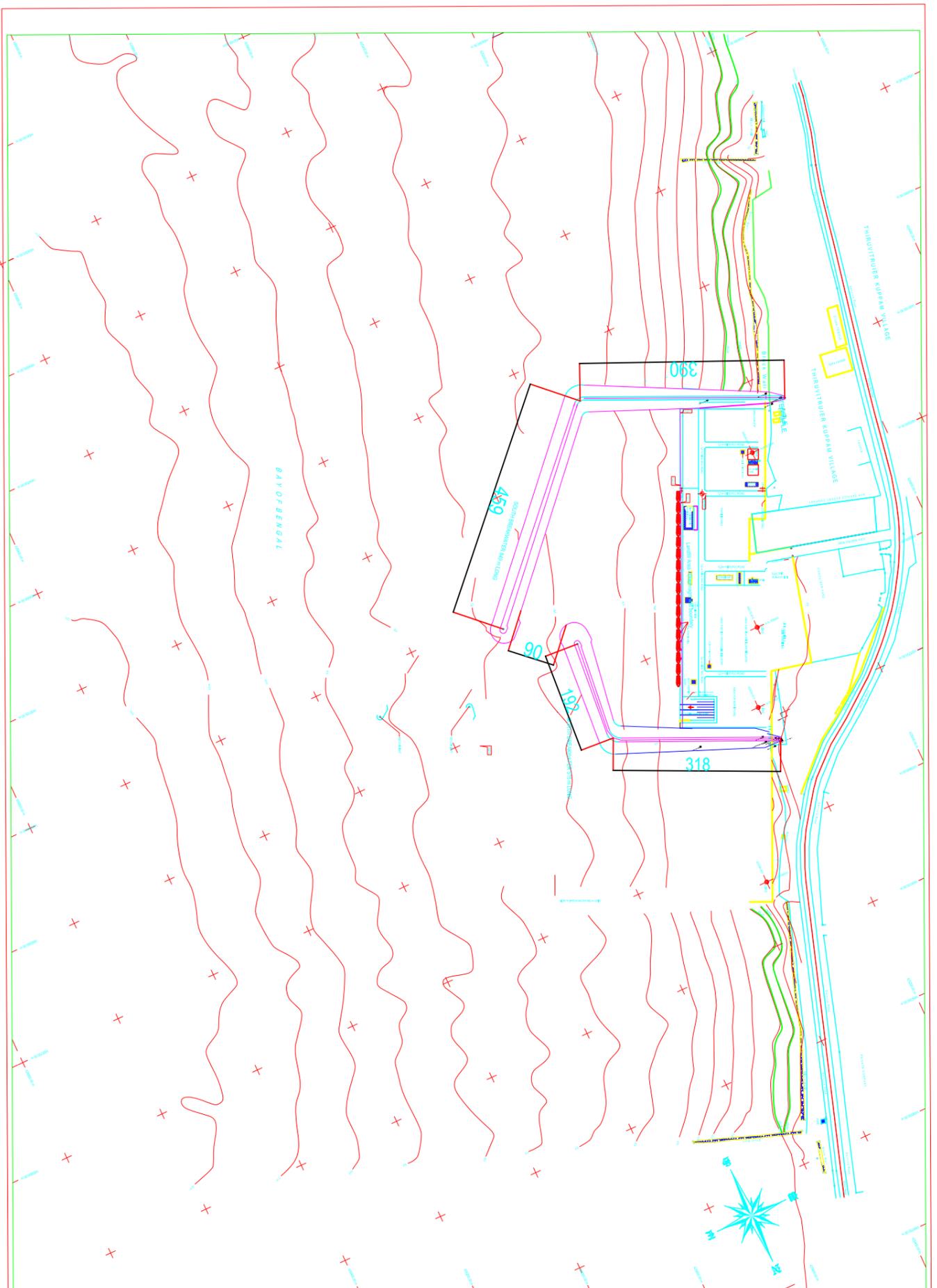
Fig.27 Phase distributions and Wave height distribution for the wave approach angle from 180[0]

ALL DIMENSIONS ARE IN 'm'

DEPARTMENT OF OCEAN ENGINEERING
IIT MADRAS

CLIENT:
FISHERIES DEPARTMENT, TAMIL NADU

PROJECT:
TUNA FISHING HARBOR AT THIRUVOTTRIYUR KUPPAM

PLATE 1 :
PROPOSED REVISED LAYOUT OF THE FISHING HARBOR

(Prof. V . SUNDAR)   (Prof.S.A.SANNASIRAJ)
DEPARTMENT   OF   OCEAN   ENGINEERING
DRAWING NO.:IITMIDOEI01   DATE : 15.07.2019   REV:00

BAY OF BENGAL

390

647

90

198

318